Lattice fermions in the Schwinger model

Geoffrey T. Bodwin
High Energy Physics Division, Argonne National Laboratory, Argonne, Illinois 60439

Eve V. Kovacs
Department of Physics, University of Illinois at Chicago, Chicago, Illinois 60680
and High Energy Physics Division, Argonne National Laboratory, Argonne, Illinois 60439
(Received 10 November 1986)

We obtain exact solutions for the continuum limit of the lattice Schwinger model, using the Lagrangian formulations of the Wilson, "naive," Kogut-Susskind, and Drell-Weinstein-Yankielowicz (DWY) lattice fermion derivatives. We examine the mass gap, the anomaly, and the chiral order parameter $\langle\bar{\psi}\psi\rangle$. As expected, our results for the Wilson formulation are consistent with those of the continuum theory and our results for the "naive" formulation exhibit spectrum doubling. In the Kogut-Susskind case, the U(1) anomaly is doubled, but $\langle\bar{\psi}\psi\rangle$ vanishes. In solving the DWY version of the model, we make use of a proposal for resumming perturbation theory due to Rabin. The Lagrangian formulation of the DWY Schwinger model displays spectrum doubling and a mass gap that is $\sqrt{2}$ times the continuum one. The U(1) anomaly graph is nonvanishing and noncovariant in the continuum limit, but has a vanishing divergence. The chiral order parameter $\langle\bar{\psi}\psi\rangle$ also vanishes.

I. INTRODUCTION

The formulation of a Lagrangian for spin-$\frac{1}{2}$ fields on a lattice has long been a problematical topic in quantum field theory. Difficulties arise in the attempt to define a lattice Lagrangian that mimics the properties of the classical (unregulated) continuum Lagrangian. In particular, inconsistencies occur when one attempts to construct a lattice action that is (1) chirally symmetric, (2) contains the correct number of fermionic degrees of freedom in the continuum limit, and (3) correctly reproduces the continuum chiral anomaly. As we shall see later, these properties are not independent. Most attempts to define a lattice theory of fermions sacrifice one or more of these properties: "naive" fermions arise from a chirally symmetric Lagrangian, but they lead to spectrum doubling and, as a consequence, a vanishing anomaly in the continuum limit; the Lagrangian for Wilson[1] fermions contains the correct number of fermionic degrees of freedom, but explicitly breaks chiral symmetry; the Kogut-Susskind[2] formulation preserves only a remnant of the complete chiral symmetry and results in spectrum doubling, though with only half the number of species of the "naive" theory. Moreover, there exist "no-go" theorems,[3–6] which state, with certain caveats, that it is impossible to introduce any field theory regulator, lattice or otherwise, that satisfies all three of the above properties.

Perhaps the most controversial lattice fermion formulation is that due to Drell, Weinstein, and Yankielowicz (DWY). This formulation has been discussed extensively in the literature,[8] and recently some variations on the basic idea have been proposed.[9] In the DWY fermion prescription, the lattice Dirac operator in momentum space is identical to the continuum operator within the Brillouin zone. However, owing to the lattice periodicity, the operator is singular on the zone boundary. As a consequence, the DWY Dirac operator is nonlocal in configuration space, and so evades some of the no-go theorems. Originally, the DWY derivative was proposed for use in a Hamiltonian setting.[7] In this paper, we investigate instead an extension of the DWY proposal to the Lagrangian case, which has been discussed by Rabin.[10] It has been claimed[10] that the DWY Lagrangian satisfies properties (1)–(3), but in general the applicability of the no-go theorem of Ninomiya and Tan is still a matter of controversy.[5] One-loop calculations using the DWY formulation in four dimensions indicate that it does not satisfy property (3) above[11] and that its singularities lead to nonlocal expressions and nonrenormalizable divergences in the vacuum polarization.[12] However, Rabin[10] has suggested that these difficulties in weak-coupling perturbation theory are the result of a spurious finite-order expansion in powers of the coupling constant. He proposes a partial resummation of the perturbation series, with the aim of regulating the DWY singularities and obtaining a well-defined expansion with the properties (1)–(3).

Our strategy in this paper is to examine the behavior of various lattice formulations for spin-$\frac{1}{2}$ particles in the context of a completely soluble model. In particular, we study electrodynamics in $1+1$ dimensions (the Schwinger model[13]), which is well known to be exactly soluble in the continuum.[13–16] We find that the lattice Schwinger models are also exactly soluble in the continuum limit to all orders in perturbation theory. In the case of the DWY version of the model, we find that it is most convenient to make use of the resummation procedure of Rabin to obtain the solution. For each lattice version of the Dirac operator, we calculate the mass gap (mass of the lowest-lying vector particle in the spectrum), the chiral anomaly,

and the vacuum expectation value of the chiral order parameter $\langle\bar{\psi}\psi\rangle$. For the naive, Wilson, and Kogut-Susskind Lagrangians, our results are consistent with the behavior expected on the basis of perturbation theory—in all cases in which this behavior was previously known. In the case of the DWY derivative, we find spectrum doubling, a vanishing anomaly, a vanishing vacuum expectation value for $\langle\bar{\psi}\psi\rangle$, and a noncovariant axial-vector current.

The remainder of this paper is organized as follows. Section II is in the nature of a review in which we introduce the rudiments of chiral symmetry and spectrum doubling on the lattice, the no-go theorems, the DWY formulation together with Rabin's resummation prescription, and the solution of the continuum Schwinger model in all-orders perturbation theory; in Sec. III we present the solutions of the lattice Schwinger model for the Wilson, naive, and Kogut-Susskind cases and also discuss the solution for a generic form of the Dirac operator on a lattice; in Sec. IV we carry out Rabin's resummation procedure and use it to obtain the solution of the DWY version of the Schwinger model; finally, in Sec. V we discuss the interpretation of our results and their implications with regard to the no-go theorems and possible formulations of the lattice fermionic action.

II. REVIEW

A. Lattice derivatives and chiral symmetry

It is well known that the straightforward transcription of the Dirac operator to the lattice, which entails the replacement of derivatives with finite differences, leads to the phenomenon of spectrum doubling. That is, in d space-time dimensions, the continuum limit of the lattice theory describes 2^d fermion species instead of just one. The occurrence of these extra species is easy to understand in terms of the zeros of the derivative function in momentum space. In general, the Fourier transform of the lattice derivative operator $D_\mu(p)$ must have the following properties: (1) $D_\mu(p)$ must be a periodic function of p with period $2\pi/a$, where a is the lattice spacing; (2) $D_\mu(p)$ must posess the correct continuum limit [$D_\mu(p)\to p_\mu$ as $a\to 0$ for fixed p_μ]. Property (1) follows from the nature of the discrete Fourier transform. Property (2) guarantees that the lattice dispersion relation for a fermion of mass m,

$$E^2=\sum_\mu D_\mu{}^2(p)+m^2 \quad \text{for } p_\mu\le\pi/a \ , \tag{2.1}$$

has the correct continuum limit. If a further restriction of continuity in p is also imposed, then periodicity implies the presence of at least one additional zero in $D_\mu(p)$ for some $p_\mu\neq 0$. Assuming that $D_\mu(p)$ is analytic, then near each zero of $D_\mu(p)$ Eq. (2.1) becomes the continuum dispersion relation, $E^2=p^2+m^2$. Hence, these additional zeros are seen to correspond to extra species in the fermion spectrum.

The simplest transcription of the continuum derivative to the lattice is the so-called "naive derivative," which, in momentum space, is given by

$$D_\mu^N(p)=\frac{1}{a}\sin p_\mu a \ . \tag{2.2}$$

In Eq. (2.2) note the presence of the additional zero crossing, which occurs at $p_\mu=\pm\pi/a$. Consequently, in two dimensions Eq. (2.1) has four minima at $(p_0,p_1)=(0,0)$, $(0,\pi/a)$, $(\pi/a,0)$, and $(\pi/a,\pi/a)$. The chiral symmetry of this theory is manifest at the classical level and remains unbroken at the quantum level because the chiralities of these extra species are such that the anomaly vanishes.

The Wilson derivative escapes the doubling problem entirely by decoupling the extra species in the continuum limit. This is achieved by introducing an extra momentum-dependent "mass" term proportional to $(1/a)\sin^2(p_\mu a/2)$ which vanishes in the continuum limit for any finite p, but gives the extra species at $p_\mu=\pi/a$ a mass proportional to $1/a$. Unfortunately, this solution of the doubling problem leads to a Lagrangian that is not chirally symmetric. This may seem to contrast with the continuum theory, in which the Lagrangian is manifestly chirally symmetric. Bear in mind, however, that, in order to obtain a well-defined continuum theory, one must introduce a regulator. The usual choices of regulators break the chiral symmetry.

The Kogut-Susskind derivative reduces the degree of doubling by thinning the fermionic degrees of freedom so that only one component of the Dirac spinor lives at each lattice site. It turns out that this is equivalent to associating the extra species with a flavor degree of freedom and amounts to adding a mass term that is proportional to a flavor matrix. The remaining spectrum doubling now occurs in flavor space. There is a corresponding remnant of chiral symmetry involving chiral rotations about one of the flavor axes. It guarantees the vanishing of the flavor-*nonsinglet* axial anomaly, but does not rule out a flavor-*singlet* [U(1)] anomaly.

Another alternative is to choose $D_\mu(p)$ to be equal to the continuum derivative within the first Brillouin zone. Such an approach was taken by Drell, Weinstein, and Yankielowicz[7] (DWY), who proposed the following lattice derivative:

$$D_\mu^{\rm DWY}(p)=p_\mu \quad \text{for } p_\mu\le\pi/a \ . \tag{2.3}$$

Since $D_\mu(p)$ must be periodic with period $2\pi/a$, the DWY derivative necessarily has discontinuities at $p_\mu=\pm\pi/a$, as shown in Fig. 1. Furthermore, owing to the presence of

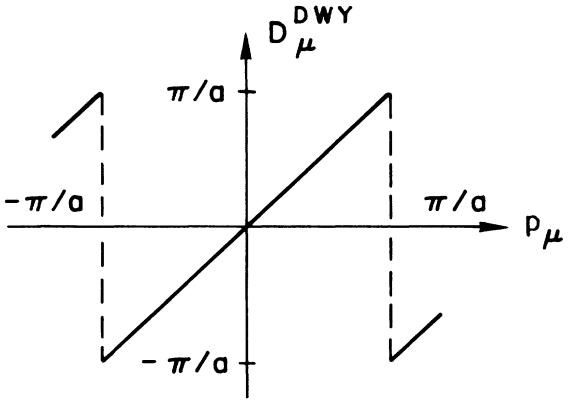

FIG. 1. The DWY derivative function in momentum space.

these discontinuities, the derivative is highly nonlocal in position space. The lattice action that results from the DWY derivative is formally chirally invariant.

The approach to the continuum limit in the DWY lattice theory has been a topic of some controversy. In particular, the mass spectrum and the value of the chiral anomaly have been discussed extensively in the literature for both the Hamiltonian[8] and the Lagrangian[10] versions of the theory. The results of Karsten and Smit in weak-coupling perturbation theory have also contributed to this discussion. Their calculations of the one-loop vacuum polarization[12] and the triangle anomaly[11] for lattice QED with DWY fermions showed that these graphs are nonlocal, not Lorentz covariant, infrared (IR) singular, and contain extra, nonrenormalizable ultraviolet (UV) divergences. Subsequently, Rabin[10] suggested that these problems did not represent an inherent difficulty with the DWY formulation, but rather, a failure of the perturbative expansion. He argued that a selective resummation of the perturbation series would render the graphs well behaved in both the IR and UV regions. In effect, the theory would provide its own cutoff, and the singularities in the DWY derivative would be smoothed out. Rabin conjectured that this procedure would be sufficient to ensure a well-behaved expansion to all orders in perturbation theory and would lead to the correct fermion spectrum and the correct anomaly in the continuum limit.

The quest for a chirally symmetric lattice theory with an undoubled spectrum and the correct anomaly has led to a number of no-go theorems.[3–6] It is well known for continuum field theories[17] that it is impossible to maintain both the gauge and chiral invariances in the presence of a regulator. A similar result for lattice theories was obtained by Nielsen and Ninomiya.[3] Their result states that it is impossible to construct a regularized chiral fermion theory with the following properties: (1) global gauge invariance; (2) different numbers of right- and left-handed species; (3) the correct anomaly; (4) local interactions; and (5) an action bilinear in the fermion fields. Karsten and Smit[6] reached similar conclusions within the context of weak-coupling perturbation theory. Finally, Ninomiya and Tan[5] have given very general topological arguments which do not rely on assumptions about the form of the lattice action. They also conclude that a lattice theory with a continuous chiral symmetry and a correct anomaly is impossible. All of the results extant in the literature for the naive, Wilson, and Kogut-Susskind lattice formulations are consistent with the above theorems. Owing to the nonlocality of the DWY derivative, that lattice formulation evades some of the earlier no-go theorems. However, the theorem of Ninomiya and Tan would seen to apply, and, indeed, the results of this paper support their conclusions.

B. The continuum Schwinger model

The exact solution of the continuum Schwinger model has been known for many years and has been discussed extensively in the literature.[13–16,18] We review here the main features of the perturbative method for obtaining the exact solution, with particular emphasis on the mass gap, the anomaly, and the expectation value of the chiral-symmetry order parameter $\langle\bar{\psi}\psi\rangle$. Note that throughout this paper we indicate all sums over indices explicitly. That is, we do not make use of a summation convention. We also choose to work in the Euclidean metric in order to be consistent with the lattice calculations that will be presented in Secs. III and IV.

1. The Ward identities

In order to facilitate the discussion, we introduce the vector and the chiral Ward identities. Consider the fermion–gauge-boson vertex $V_\mu(p,l)$, where p and l denote the incoming fermion and gauge-boson momenta, respectively, and m denotes the fermion mass, which will eventually be set to zero. By rewriting $\not{l}$ as $(\not{p}+\not{l}+m)-(\not{p}+m)$, we obtain the well-known Feynman identity

$$\begin{aligned} S_F(p+l)\sum_\mu l_\mu V_\mu(p,l)S_F(p) &= \frac{1}{\not{p}+\not{l}+m}(-e)[(\not{p}+\not{l}+m)-(\not{p}+m)]\frac{1}{\not{p}+m} \\ &= (-e)[S_F(p)-S_F(p+l)]\ , \end{aligned} \tag{2.4}$$

where

$$S_F(p)=\frac{1}{\not{p}+m} \tag{2.5}$$

is the Feynman propagator for the fermion field. Hence, the contraction $\sum_\mu l_\mu V_\mu(p,l)$ can be rewritten as the difference of two *scalar* vertices with the fermion propagators canceled on the left- and right-hand sides, respectively. This is shown graphically in Fig. 2, where the arrowhead on the incoming gauge boson denotes the momentum contraction, the open circles denote scalar interactions, and the slashes on the fermion lines denote the cancellation of the propagators. A similar result can be derived for the axial-vector vertex $V_\mu^5(p,l)$, which we obtain by making the replacement

$$\gamma_\mu \rightarrow \gamma_\mu\gamma_5$$

in the corresponding vector vertex. Throughout this paper we use the convention that γ_5 appears on the right-hand side (RHS) of a vertex with the fermion momentum flowing from right to left. We use a 5 to denote the axial vertices in Feynman diagrams and algebraic expressions. The Feynman identity for the axial-vector vertex is obtained by rewriting $\not{l}\gamma_5$ as

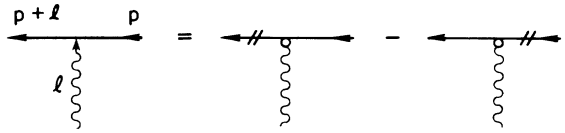

FIG. 2. Graphical representation of the vector Ward identity for the lepton-photon vertex. As explained in the text, the arrow indicates the contraction of the photon momentum into the Lorentz index of the vertex, the open circle indicates a scalar vertex ($-e\gamma_\mu \rightarrow -e$), and the hash marks on a propagator indicate that the propagator is canceled.

$$S_F(p+l)\sum_\mu l_\mu V^5_\mu(p,l)S_F(p)=\frac{1}{\not p+\not l+m}(-e)[(\not p+\not l+m)\gamma_5+\gamma_5(\not p+m)-2m\gamma_5]\frac{1}{\not p+m}$$

$$=(-e)[\gamma_5 S_F(p)+S_F(p+l)\gamma_5+S_F(p+l)(-2m\gamma_5)S_F(p)]\ . \tag{2.6}$$

Equation (2.6) is depicted in graphical form in Fig. 3.

2. *The mass gap*

The mass gap for the case $m=0$ is easy to calculate once it is realized that all graphs which contain fermion loops with more than two photon vertices vanish. The most general proof of this result relies on the vector and axial-vector Ward identities established above. Let $\Gamma_{\mu_1\cdots\mu_N}(l_1,\ldots,l_N)$ denote the graph shown in Fig. 4 with N incoming photons carrying moments $l_1,\ldots,l_N$. The photons are labeled in a clockwise fashion around the loop. Similarly, $\Gamma^5_{\mu_1\cdots\mu_N}(l_1,\ldots,l_N)$ denotes the analogous quantity with an additional γ_5 coupling at the μ_1 vertex. For $N>2$, each of the graphs $\Gamma_{\mu_1\cdots\mu_N}(l_1,\ldots,l_N)$ or $\Gamma^5_{\mu_1\cdots\mu_N}(l_1,\ldots,l_N)$ is absolutely convergent and hence requires no regulator. The complete set of Feynman graphs in a given order consists of a sum over all distinct permutations of the photon connections. This set of graphs can be decomposed into disjoint subsets labeled according to the relative positions of photons 2 through N. All of the graphs in a given subset are obtained by summing over all connections of photon 1. Let us consider one such subset

$$\Gamma_{\mu_1\cdots}=\sum_{\text{connections}}\Gamma_{\mu_1\cdots}$$

$$=\Gamma_{\mu_1\mu_2\cdots\mu_N}$$

$$+\Gamma_{\mu_2\mu_1\mu_3\cdots\mu_N}+\ldots+\Gamma_{\mu_2\cdots\mu_{N-1}\mu_1\mu_N}\ . \tag{2.7}$$

The same rearrangement may also be performed on the corresponding axial graph $\Gamma^5_{\mu_1\cdots}=\sum_{\text{connections}}\Gamma^5_{\mu_1\cdots}$. Now we contract these sums over connections with the external momentum l_1. Provided that one can make a finite shift of the loop momentum, it can be shown by repeated application of Eqs. (2.4) and (2.6) that

$$\sum_{\mu_1}(l_1)_{\mu_1}\Gamma_{\mu_1\cdots}=0\ , \tag{2.8a}$$

$$\sum_{\mu_1}(l_1)_{\mu_1}\Gamma^5_{\mu_1\cdots}=0\ . \tag{2.8b}$$

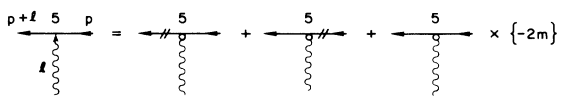

FIG. 3. Graphical representation of the axial-vector Ward identity for the fermion-axial photon vertex. As explained in the text, our convention is that the γ_5 appears on the side of the vertex into which the fermion momentum flows. The remaining diagrammatic symbols have the same meaning as in Fig. 2.

These finite shifts of loop momentum are valid for $N>2$, since the individual terms obtained from the application of Eqs. (2.4) and (2.6) are, at worst, logarithmically divergent. Note that Eq. (2.8b) holds only in the case of massless fermions. In two dimensions the γ matrices satisfy the additional useful relationship

$$\gamma_\mu\gamma_5=-\sum_\nu\epsilon_{\mu\nu}\gamma_\nu\ , \tag{2.9}$$

where we have used the conventions $\{\gamma_\mu,\gamma_\nu\}=-2\delta_{\mu\nu}$, $\gamma_5=\gamma_0\gamma_1$, and $\epsilon_{01}=1$. Hence,

$$\Gamma^5_{\mu_1\cdots}=-\sum_\nu\epsilon_{\mu_1\nu}\Gamma_{\nu\cdots}\ , \tag{2.10}$$

and Eqs. (2.8a) and (2.8b) become

$$(l_1)_0\Gamma_{0\cdots}+(l_1)_1\Gamma_{1\cdots}=0\ , \tag{2.11a}$$

$$(l_1)_0\Gamma_{1\cdots}-(l_1)_1\Gamma_{0\cdots}=0\ . \tag{2.11b}$$

Since the momentum l_1 is arbitrary, the only solution to Eqs. (2.11a) and (2.11b) is

$$\Gamma_{\mu_1\cdots}\equiv 0\ . \tag{2.12}$$

That is, since the divergence and curl of $\Gamma_{\mu_1\cdots}$ vanish, $\Gamma_{\mu_1\cdots}$ itself must vanish. This completes the proof. Note that it is possible to join up two or more of the incoming photons and dress them up in any desired way without altering the above conclusions. The only graph which evades the preceding analysis is the vacuum-polarization graph $\Pi_{\mu\nu}(l)$ depicted in Fig. 5(a). Since this graph has only two external legs and no internal photon lines, the loop integral is superficially logarithmically divergent. The separate terms resulting from Eqs. (2.4) and (2.6) are then linearly divergent, so that a shift of the loop momentum changes the value of the integral. The introduction of a regulator that renders the graph finite

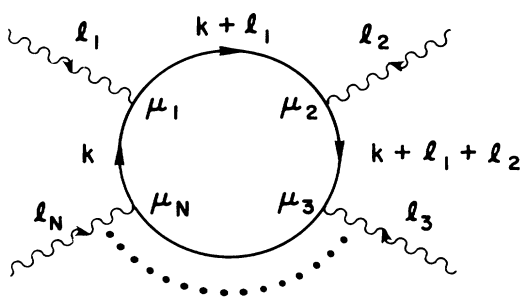

FIG. 4. A fermion loop with N attached photons. The μ_i are the Lorentz indices of the vector vertices, the l_i are the external photon momenta, and k is the loop momentum.

necessarily breaks either gauge invariance or chiral invariance.[17] Hence, either Eq. (2.8a) or (2.8b) is no longer true and the proof fails.

In order to evaluate $\Pi_{\mu\nu}(l)$ we must, therefore, select a scheme for regulating the loop integral. We choose the Pauli-Villars method because the resulting expressions are very similar to the ones that ultimately arise in the lattice calculations presented in Secs. III and IV. This method entails subtracting from the original integrand a quantity obtained by replacing the fermion mass m with a regulator mass M [see Fig. 5(b)]. Eventually, we take $M\to\infty$. Then, the regulated vacuum polarization is given by

$$\Pi^{\rm PV}_{\mu\nu}(l,m)=\lim_{M\to\infty}(-e^2)\int\frac{d^2k}{(2\pi)^2}\mathrm{Tr}\left[\frac{1}{k+l+m}\gamma_\mu\frac{1}{k+m}\gamma_\nu-\frac{1}{k+l+M}\gamma_\mu\frac{1}{k+M}\gamma_\nu\right], \tag{2.13}$$

where the notation follows that of Fig. 5. Note that since M is assumed to be large, we may neglect l in the denominator of the second term of Eq. (2.13). Combining denominators by using Feynman parameters and discarding terms that are odd in k_0 or k_1, we obtain an expression that is finite in the $M\to\infty$ limit. In fact, the expression is independent of M. As usual, the constraint of gauge invariance has resulted in the cancellation of the most divergent terms in the amplitude. Thus, the Schwinger model requires no renormalization. The remaining expression consists of elementary integrals, which we evaluate for $m=0$ to obtain

$$\Pi^{\rm PV}_{\mu\nu}(l,0)=-\frac{e^2}{\pi}\left[\delta_{\mu\nu}-\frac{l_\mu l_\nu}{l^2}\right]=-\frac{e^2}{\pi}G_{\mu\nu}\ . \tag{2.14}$$

We can obtain the complete photon propagator with external legs amputated (the current-current correlation function $J_{\mu\nu}$) by summing to all orders the series of graphs shown in Fig. 6:

$$\begin{aligned}J_{\mu\nu}(l)&=\int d^2x\, e^{il\cdot x}\langle j_\mu(x)j_\nu(0)\rangle\\&=\frac{-e^2}{\pi}G_{\mu\nu}+\left[\frac{-e^2}{\pi}\right]^2\frac{G_{\mu\nu}}{l^2}+\cdots\\&=-\frac{e^2}{\pi}G_{\mu\nu}\frac{l^2}{l^2+e^2/\pi}\ .\end{aligned} \tag{2.15}$$

Hence, we have recovered the famous result that the Schwinger model with a single massless fermion contains a massive vector particle with a mass $e/\sqrt{\pi}$.

The N_f flavor model has also been studied extensively.[14] In general, the particle spectrum is more complicated and, in the case where the fermions are allowed to have masses, no solution of the model exists for any value of N_f. Restricting the fermions to zero mass, one can clearly form $N_f{}^2$ massless scalar states. Because each flavor can contribute equally to the vacuum polarization, the vector mass is $\sqrt{N_f}e/\sqrt{\pi}$. In general, if the vacuum polarization is of the form

$$\Pi_{\mu\nu}(l)=N_\Pi\left[-\frac{e^2}{\pi}\left[\delta_{\mu\nu}-\frac{l_\mu l_\nu}{l^2}\right]\right], \tag{2.16}$$

then the mass gap is given by

$$\mu=\sqrt{N_\Pi}\frac{e}{\sqrt{\pi}}\ . \tag{2.17}$$

3. The anomaly

The anomaly is the divergence of the amplitude $A_{\mu\nu}(l,0)$ that one obtains by making the replacement $\gamma_\mu\to\gamma_\mu\gamma_5$ in $\Pi_{\mu\nu}(l,0)$. As in the case of the vacuum polarization, $A_{\mu\nu}(l,m)$ is not defined until it is regulated. Again we choose a Pauli-Villars scheme. The regulated quantity is represented by Fig. 5, except that γ_5's are to be inserted, as previously described, to the right of the γ_μ's at the vertices with index μ. The details of the computation are almost identical to those given in Sec. II B 2 for $\Pi_{\mu\nu}$. Taking $m=0$, we obtain

$$A^{\rm PV}_{\mu\nu}(l,0)=\frac{e^2}{\pi}\left[\epsilon_{\mu\nu}-\frac{\sum_\alpha\epsilon_{\mu\alpha}l_\alpha l_\nu}{l^2}\right]. \tag{2.18}$$

The anomaly is then

$$\sum_\mu l_\mu A^{\rm PV}_{\mu\nu}(l,0)=\frac{e^2}{\pi}\sum_\mu l_\mu\epsilon_{\mu\nu}\ . \tag{2.19}$$

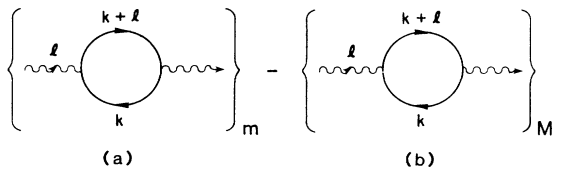

FIG. 5. (a) The Feynman graph that gives the vacuum-polarization contribution in the continuum Schwinger model and (b) the corresponding Pauli-Villars subtraction.

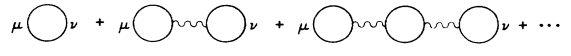

FIG. 6. The geometric series of vacuum-polarization bubbles that gives the current-current correlation function $J_{\mu\nu}$.

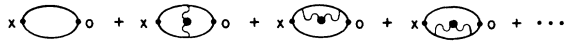

FIG. 7. The expansion of $G(x,0)$ according to the number of complete photon propagators. The dots on the wavy line indicate the complete propagator $K_{\mu\nu}$.

4. $\langle\bar{\psi}\psi\rangle$

The expansion value of the chiral order parameter $\langle\bar{\psi}\psi\rangle$ has been calculated both directly, in the fermionic version of the model,[18] and indirectly, in the bosonized version.[14] Note that $\bar{\psi}\psi$ has zero expectation value in the perturbative vacuum. However, it is possible to compute perturbatively the expectation value of $\bar{\psi}\psi$ in the nonperturbative vacuum by considering the four-point function $G(x,0)$ defined by

$$G(x,0)=\langle 0\,|\,\bar{\psi}(x)\psi(x)\bar{\psi}(0)\psi(0)\,|\,0\rangle\ , \tag{2.20a}$$

where $|0\rangle$ denotes the perturbative vacuum. At large x, $G(x,0)$ can be related to the expectation value of $\bar{\psi}\psi$ in the nonperturbative vacuum:

$$\lim_{x\to\infty} G(x,0)=\tfrac{1}{2}\,|\,\langle\bar{\psi}\psi\rangle\,|^2\ . \tag{2.20b}$$

The details leading to Eq. (2.20b) are given in the Appendix.

We now present the perturbative calculation of $G(x,0)$. The lowest-order diagrams which contribute to $G(x,0)$ are shown in Fig. 7. The vector interactions at the photon vertices may be rewritten as pseudoscalar interactions by making use of some special properties of two-dimensional gauge theories. Consider the case of a complete photon propagator $K_{\mu\nu}(l)$ connecting two fermion lines, as shown in Fig. 8. By using the two-dimensional expression for the transversality projector,

$$\delta_{\mu\nu}-\frac{l_\mu l_\nu}{l^2}=\sum_{\alpha,\beta}\frac{-\epsilon_{\mu\alpha}l_\alpha l_\beta\epsilon_{\beta\nu}}{l^2}\ , \tag{2.21}$$

we can rewrite $K_{\mu\nu}(l)$ in the Landau gauge as

$$\begin{aligned}K_{\mu\nu}(l)&=\left[\delta_{\mu\nu}-\frac{l_\mu l_\nu}{l^2}\right]\frac{1}{l^2+\mu^2}\\&=-\sum_{\alpha,\beta}\epsilon_{\mu\alpha}l_\alpha l_\beta\epsilon_{\beta\nu}\frac{1}{l^2(l^2+\mu^2)}\\&=-\sum_{\alpha,\beta}\epsilon_{\mu\alpha}l_\alpha l_\beta\epsilon_{\beta\nu}K(l)\ ,\end{aligned} \tag{2.22}$$

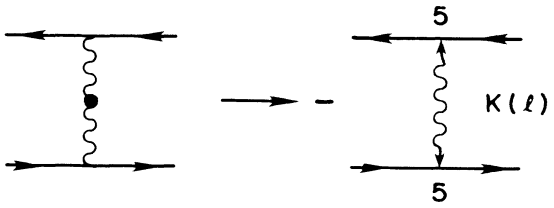

FIG. 8. Graphical representation of Eq. (2.24), which gives an equivalent expression—valid in two dimensions—for the complete photon propagator in the Landau gauge.

where

$$K(l)=\frac{1}{l^2(l^2+\mu^2)}\ . \tag{2.23}$$

Including the vector interactions at the vertices and making use of the γ-matrix rearrangement of Eq. (2.9), we find that

$$\begin{aligned}\sum_{\mu,\nu}\gamma_\mu\otimes\gamma_\nu K_{\mu\nu}(l)&=-\sum_{\mu,\nu,\alpha,\beta}\gamma_\mu\epsilon_{\mu\alpha}l_\alpha\otimes l_\beta\epsilon_{\beta\nu}\gamma_\nu K(l)\\&=\sum_{\mu,\nu}l_\mu\gamma_\mu\gamma_5\otimes l_\nu\gamma_\nu\gamma_5 K(l)\ .\end{aligned} \tag{2.24}$$

Hence, each photon propagator and its accompanying vertices may be replaced with a modified photon propagator, whose momentum dependence is $K(l)$, and accompanying axial-vector vertices, whose Lorentz indices are contracted with the photon momentum indices. This is illustrated graphically in Fig. 8. The minus sign on the RHS of the figure arises because the photon momentum l flows into one vertex and out of the other vertex. The point in performing these manipulations is that we can now simplify the calculation by applying the axial-vector Ward identity, Eq. (2.6) to the diagrams of Fig. 7. The result is shown in Fig. 9. Note that in these diagrams the momentum dependence of the photon propagator with momentum k is given by $K(k)$ and the vertices are now scalar vertices, the γ matrices having been removed by the Ward identity rearrangement. Evaluating the diagrams in coordinate space we obtain

$$\begin{aligned}G(x,0)&=\mathrm{Tr}[\tilde{S}_F(x)]^2\{1+4e^2[\tilde{K}(0)-\tilde{K}(x)]+\cdots\}\\&=\mathrm{Tr}[\tilde{S}_F(x)]^2\left[1+2e^2\int\frac{d^2k}{(2\pi)^2}\frac{|1-e^{ik\cdot x}|^2}{k^2(k^2+\mu^2)}+\cdots\right]=\frac{1}{2\pi^2x^2}[1+P(x)\cdots]\ ,\end{aligned} \tag{2.25}$$

where the tildes denote Fourier transforms. The series exponentiates and hence $G(x,0)$ is given by

$$G(x,0)=\frac{1}{2\pi^2x^2}e^{P(x)}=\frac{1}{2\pi^2x^2}\exp\left[\frac{2e^2}{\pi\mu^2}[\gamma_E+\ln(\tfrac{1}{2}\mu x)+K_0(\mu x)]\right]\ , \tag{2.26}$$

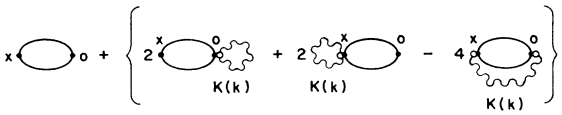

FIG. 9. The result of applying the axial-vector Ward identity of Fig. 3 to the series of Fig. 7.

where γ_E is Euler's constant and K_0 is the modified Bessel function. Evaluating Eq. (2.26) at large x and recalling that $\mu^2=N_\Pi e^2/\pi$, we obtain

$$G(x,0)\underset{x\to\infty}{\longrightarrow}\frac{1}{2\pi^2x^2}(\tfrac{1}{2}\mu x)^{2e^2/\pi\mu^2}\exp\left[\frac{2e^2\gamma_E}{\pi\mu^2}\right]$$

$$=\frac{1}{2\pi^2}(\tfrac{1}{2}\mu)^{2/N_\Pi}x^{(2/N_\Pi)-2}\exp\left[\frac{2\gamma_E}{N_\Pi}\right] \quad (2.27a)$$

$$\underset{x\to\infty}{\longrightarrow}\begin{cases}\dfrac{\mu^2}{8\pi^2}e^{2\gamma_E} & \text{for } N_\Pi=1\ ,\\ 0 & \text{for } N_\Pi>1\ .\end{cases} \quad (2.27b)$$

We see from Eq. (2.27b) that $\langle\bar\psi\psi\rangle$ develops a vacuum expectation value only for the case of one flavor. In all other cases $\langle\bar\psi\psi\rangle$ remains zero:

$$\langle\bar\psi\psi\rangle=\begin{cases}\dfrac{\mu^2}{4\pi^2}e^{2\gamma_E} & \text{for } N_\Pi=1\ ,\\ 0 & \text{for } N_\Pi>1\ .\end{cases} \quad (2.28)$$

III. THE SCHWINGER MODEL ON A LATTICE

In this section we discuss the solution of the Schwinger model for the cases of the Wilson, naive, and Kogut-Susskind fermionic actions on a Euclidean lattice. The procedures involved are somewhat simpler technically for these cases than for the DWY action. However, many of the techniques that we develop here will be useful in discussing the DWY version of the model. For the naive and Wilson actions we can test our results against the lore that is based on finite-order weak-coupling perturbation theory. In the case of the Kogut-Susskind action, we derive some results that have not been described elsewhere in the literature.

A. Propagators and vertices

In the following equations, a denotes the lattice spacing, a_μ denotes a unit lattice vector in the μ direction, m denotes the fermion mass (which we will eventually set to zero), and the γ_μ are the Euclidean versions of the Dirac matrices:

$$\{\gamma_\mu,\gamma_\nu\}=-2\delta_{\mu\nu}\ , \quad (3.1a)$$

$$\gamma_5=\gamma_0\gamma_1\ . \quad (3.1b)$$

The fermionic parts of the various Euclidean lattice actions for the Wilson[1] and naive[10] cases are, respectively,

$$I^W=-a^2\sum_{x,\mu}\bar\psi(x)\frac{1}{i}\gamma_\mu\frac{1}{2a}[\psi(x+a_\mu)-\psi(x-a_\mu)]$$

$$-a^2\sum_{x,\mu}\bar\psi(x)\frac{1}{2a}[\psi(x+a_\mu)+\psi(x-a_\mu)-2\psi(x)]$$

$$-a^2\sum_x m\bar\psi(x)\psi(x) \quad (3.2a)$$

and

$$I^N=-a^2\sum_{x,\mu}\bar\psi(x)\frac{1}{i}\gamma_\mu\frac{1}{2a}[\psi(x+a_\mu)-\psi(x-a_\mu)]$$

$$-a^2\sum_x m\bar\psi(x)\psi(x)\ . \quad (3.2b)$$

In the Kogut-Susskind[2] case the original Lagrangian can be manipulated into the form[19]

$$I^{KS}=-a^2\sum_{x,\mu}\bar\psi(x)\frac{1}{i}\gamma_\mu\frac{1}{2a}[\psi(x+a_\mu)-\psi(x-a_\mu)]$$

$$-a^2\sum_{x,\mu}\bar\psi(x)\gamma_5(-\tau_\mu)\frac{1}{2a}$$

$$\times[\psi(x+a_\mu)+\psi(x-a_\mu)-2\psi(x)]$$

$$-a^2\sum_x m\bar\psi(x)\psi(x)\ . \quad (3.2c)$$

In this case ψ is a vector in the two-dimensional flavor space as well as in the Dirac matrix space; the τ_μ are the first and second generators of the SU(2)-flavor group in the fundamental representation ($\tau_\mu^2=1$). The corresponding momentum-space Feynman-Dirac propagators $S_F(p)$ are easily obtained by Fourier transforming the fermionic actions. These are

$$S_F^W(p)=\left[\sum_\mu\frac{1}{a}(\gamma_\mu\sin p_\mu a+2\sin^2\tfrac{1}{2}p_\mu a)+m\right]^{-1} \quad (3.3a)$$

for the Wilson case,

$$S_F^N(p)=\left[\sum_\mu\frac{1}{a}(\gamma_\mu\sin p_\mu a)+m\right]^{-1} \quad (3.3b)$$

for the naive case, and

$$S_F^{KS}(p)=\left[\sum_\mu\frac{1}{a}(\gamma_\mu\sin p_\mu a-2\tau_\mu\gamma_5\sin^2\tfrac{1}{2}p_\mu a)+m\right]^{-1} \quad (3.3c)$$

for the Kogut-Susskind case. We write these propagators generically as

$$S_F(p)=\left[\sum_\mu\nabla_\mu(p)+m\right]^{-1}$$

$$=\left[\left[\sum_\mu\gamma_\mu D_\mu(p)\right]+M_\mu(p)+m\right]^{-1}\ , \quad (3.4)$$

where $D_\mu(p)$ and $M_\mu(p)$ denote the fermion derivative function and the momentum-dependent "mass terms," respectively.

Interactions with the photon field can be introduced in

a gauge-invariant manner by implementing the lattice version of minimal substitution:

$$\psi(x\pm a_\mu)\rightarrow\psi(x\pm a_\mu)\exp[\pm ieaA_\mu(x)]\ , \tag{3.5}$$

where $A_\mu(x)$ is the gauge field and e is the gauge coupling constant. An expansion of the action in powers of the coupling constant then leads to the set of interaction vertices shown in Fig. 10. Note that there is an infinite set of seagull-type interactions. The Feynman rules for the one- and two-photon vertices are, respectively,

$$V_\mu^{(1)W}(p,l)=-e[\gamma_\mu\cos(p_\mu+\tfrac{1}{2}l_\mu)a+\sin(p_\mu+\tfrac{1}{2}l_\mu)a]\ , \tag{3.6a}$$

$$V_{\mu\nu}^{(2)W}(p,l)=ae^2\delta_{\mu\nu}[\gamma_\mu\sin(p_\mu+\tfrac{1}{2}l_\mu)a-\cos(p_\mu+\tfrac{1}{2}l_\mu)a] \tag{3.6b}$$

for the Wilson case,

$$V_\mu^{(1)N}(p,l)=-e\gamma_\mu\cos(p_\mu+\tfrac{1}{2}l_\mu)a\ , \tag{3.6c}$$

$$V_{\mu\nu}^{(2)N}(p,l)=ae^2\delta_{\mu\nu}\gamma_\mu\sin(p_\mu+\tfrac{1}{2}l_\mu)a \tag{3.6d}$$

for the naive case, and

$$V_\mu^{(1)\mathrm{KS}}(p,l)=-e[\gamma_\mu\cos(p_\mu+\tfrac{1}{2}l_\mu)a-\tau_\mu\gamma_5\sin(p_\mu+\tfrac{1}{2}l_\mu)a]\ , \tag{3.6e}$$

$$V_{\mu\nu}^{(2)\mathrm{KS}}(p,l)=ae^2\delta_{\mu\nu}[\gamma_\mu\sin(p_\mu+\tfrac{1}{2}l_\mu)a+\tau_\mu\gamma_5\cos(p_\mu+\tfrac{1}{2}l_\mu)a] \tag{3.6f}$$

for the Kogut-Susskind case. The lattice momentum is given by

$$d_\mu(p)\equiv(2/a)\sin\tfrac{1}{2}p_\mu a\ , \tag{3.7}$$

which is equal to the momentum p_μ in the continuum limit $a\rightarrow 0$. By contracting the lattice momentum into one index of a vertex $V_\mu^{(n)}\ldots$, we can obtain an expression involving only lower-order vertices and propagators.

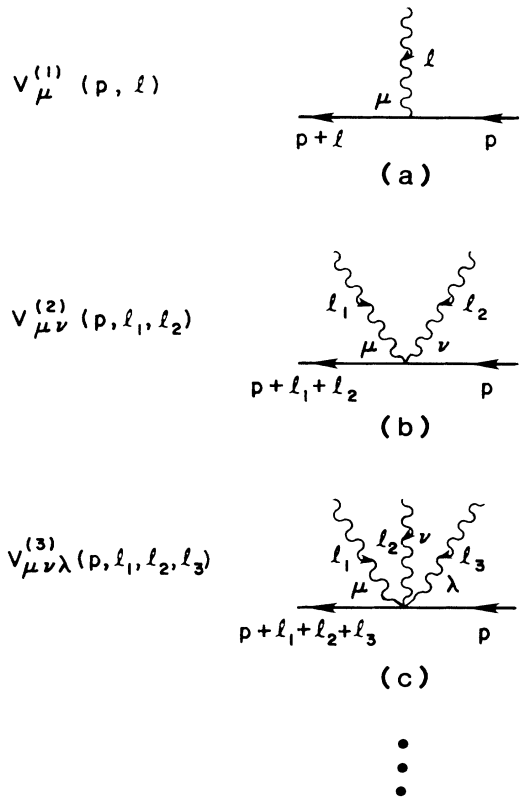

FIG. 10. The lattice vertices $V_\mu^{(1)}(p,l)$, $V_{\mu\nu}^{(2)}(p,l_1,l_2)$, and $V_{\mu\nu\lambda}^{(3)}(p,l_1,l_2,l_3)$. The labels μ,ν,λ denote the Lorentz indices of the vertices, p is the fermion momentum, and the l_i are the photon momenta.

These lattice Ward identities are analogous to the Feynman identity in the continuum and are a consequence of gauge invariance. They are shown in Fig. 11.

An alternative procedure is to derive the Feynman rules for the vertices by starting with a given lattice propagator and demanding that the vertices satisfy the graphical Ward identities. For the generic propagator given in Eq. (3.4), the Ward identity of Fig. 11(a) gives

$$V_\mu^{(1)}(p,l)=-e\frac{\nabla_\mu(p+l)-\nabla_\mu(p)}{d_\mu(l)} \tag{3.8a}$$

and the Ward identity of Fig. 11(b) gives

$$V_{\mu\nu}^{(2)}(p,l_1,l_2)=-e^2\delta_{\mu\nu}\frac{\nabla_\mu(p+l_1+l_2)-\nabla_\mu(p+l_2)-\nabla_\mu(p+l_1)+\nabla_\mu(p)}{d_\mu(l_1)d_\mu(l_2)}\ . \tag{3.8b}$$

In general we have the relation between the n-photon and the $(n+1)$-photon vertex [Fig. 11(c)]:

$$V_{\mu_1\cdots\mu_{n+1}}^{(n+1)}(p,l_1,\ldots,l_{n+1})=e\delta_{\mu_n,\mu_{n+1}}\frac{V_{\mu_1\cdots\mu_n}^{(n)}(p+l_{n+1},l_1,\ldots,l_n)-V_{\mu_1\cdots\mu_n}^{(n)}(p,l_1,\ldots,l_n)}{d_{\mu_{n+1}}(l_{n+1})}\ . \tag{3.8c}$$

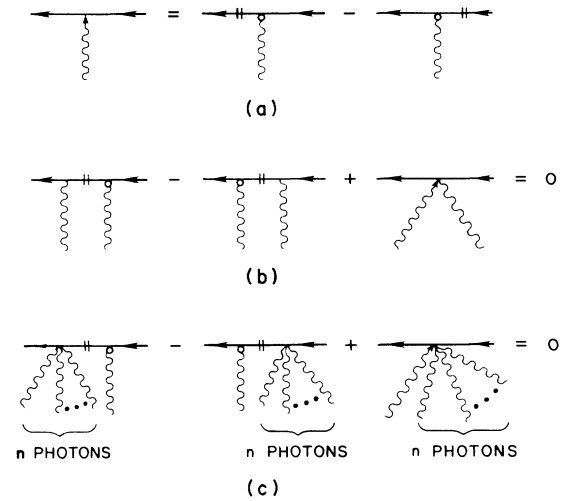

FIG. 11. The lattice vector Ward identities for (a) one photon, (b) two photons, and (c) $n+1$ photons. The open circle indicates a scalar vertex ($V_\mu^{(1)} \rightarrow -e$).

One can also define an axial-vector current on the lattice and derive Ward identities for the resulting vertices. Here, we find it convenient to define the axial-vector vertices so that they are obtained by making the replacement

$$\gamma_\mu \rightarrow \gamma_\mu \gamma_5$$

in the corresponding vector vertices. (Note that this is not the only possible definition for the lattice chiral current. See, for example, Ref. 8.) The graphical Ward identities for the axial-vector vertices are shown in Fig. 12.

B. General procedure for the solution of the lattice models

Let us now discuss the procedure for solving the lattice versions of the Schwinger model. Our discussion will be couched in terms of the generic fermion propagator of Eq.

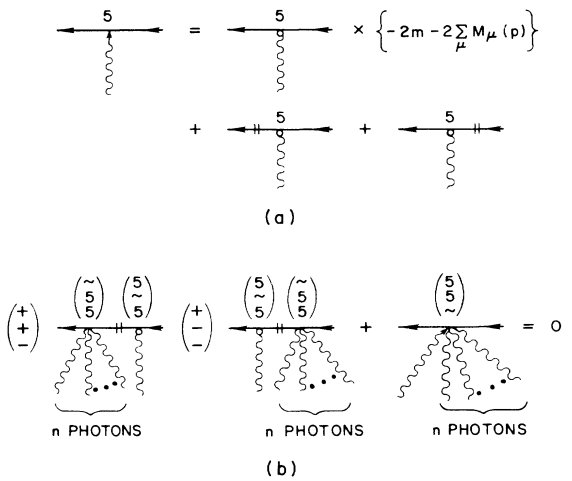

FIG. 12. The lattice axial-vector Ward identities for (a) one photon and (b) $n+1$ photons. The open circle indicates a scalar vertex ($V_\mu^{(1)} \rightarrow -e$).

(3.4). In this section we will assume that $\nabla_\mu(p)$ is an analytic function of $p_\mu a$ for all fixed a and in the limit $a \rightarrow 0$. This is the case for the naive, Wilson, and Kogut-Susskind derivatives. For the DWY derivative, we will need a somewhat more elaborate procedure than the one to be presented in this section.

The various propagators of Eq. (3.3) all tend to the continuum propagator in the limit $a \rightarrow 0$. Of course, one cannot simply take the limit $a \rightarrow 0$ in the propagators when they are a part of an expression involving an integration over loop momenta. Since the loop momenta range from $-\pi/a$ to π/a, $p_\mu a$ in the arguments of the propagators can become of ~ 1, so that a simple expansion in the explicit powers of a is not valid. Instead, one must work out the power counting for the complete integral. As we shall see, in the limit $a \rightarrow 0$, the leading contributions from loop integrals come from the regions near the poles in the propagators. All of the lattice propagators have a pole near $p_\mu = 0$, by virtue of the fact that they go over to the continuum propagator in the limit $a \rightarrow 0$. In addition, the naive propagator [Eq. (3.3b)] has a pole at $p_\mu = \pm \pi/a$. Near the poles at $p_\mu = 0$, the propagators and vertices are approximately equal to the continuum ones; near the pole at $p_\mu = \pm \pi/a$, the naive propagators and vertices are (up to a shift in momentum of π/a) equal to the continuum ones with $\gamma_i \rightarrow -\gamma_i$. We give the name linear regions to these regions near the propagator poles in which the linear approximation is good. Within the linear regions, the higher-order terms in the Taylor-series expansions of the propagators and vertices are suppressed relative to the linear terms in the limit $a \rightarrow 0$. The degree of suppression depends on the particular graph and on the form of the lattice derivative. We expect to obtain a contribution proportional to the continuum contribution from each of the linear regions. In the case of the naive derivative, the extra contributions from the linear regions near $p_\mu = \pi/a$ produce the doubling phenomenon.

1. *Higher-order loops*

Let us work out the contribution of a single fermion loop with N external photons in the limit $a \rightarrow 0$. We analyze the situation for internal photons later. Consider first the case for which the power-counting arguments are simplest, namely, $N > 2$. The corresponding continuum graphs lead to integrals that are absolutely convergent; i.e., they need no regulators. Thus, we expect the lattice expressions to go over to continuum ones in the limit $a \rightarrow 0$. In order to demonstrate this, we estimate the order of magnitude of the Feynman integral. Our aim is to show that only the linear regions contribute as $a \rightarrow 0$. Since we wish to focus on the a dependence of the amplitudes, here, and in all succeeding discussions of orders of magnitude, we omit factors of e and drop the external momenta in the propagators and vertices. The external momenta provide infrared cutoffs for the integrals, but our concern is with the ultraviolet behavior. As a consequence of these simplifications, some expressions may not appear to be dimensionally correct. In more complete expressions, the missing dimensions would, of course, be made up by powers of e and the external momenta.

Consider first the situation in which none of the photon attachments is a seagull (Fig. 4). Each of the fermion propagators (Eq. 3.4) gives a factor whose magnitude is

$$\frac{1}{\nabla(k)} \equiv \frac{1}{\left[\sum_{\mu} |\nabla_{\mu}(k)|^2\right]^{1/2}} = \frac{a}{a\nabla(k)} . \tag{3.9}$$

Note that the dimensionless quantity $a\nabla(k)$ is ~ 1 except near the poles in the fermion propagators. Each of the vertices supplies a factor $V^{(1)}$. The range of integration is $-\pi/a$ to π/a for each of the integration variables k_0 and k_1, so the range contributes an overall factor a^{-2} to the order of magnitude. Thus, the upper bound on the contribution to the graph from any interval in k can be obtained by considering the quantity

$$\frac{a^{N-2}}{[a\nabla(k)]^N} |V^{(1)}|^N . \tag{3.10}$$

We approximate $|V^{(1)}|$ by its maximum, which is ~ 1. Then, the condition for the loop to contribute in the limit $a \to 0$ is

$$\frac{a^{N-2}}{[a\nabla(k)]^N} \gtrsim 1 . \tag{3.11a}$$

That is,

$$|a\nabla| \lesssim a^{(N-2)/N} . \tag{3.11b}$$

For $N>2$, the RHS of Eq. (3.11b) goes to zero as $a \to 0$; therefore, the LHS must also go to zero if Eq. (3.11b) is to be satisfied. This happens only for $k_\mu a$ near 0 or π. Specifically, we must have

$$|k_\mu a| \lesssim a^{(N-2)/N}$$

or (3.11c)

$$|k_\mu a| - \pi \lesssim a^{(N-2)/N} .$$

In these regions the higher-order terms in the Taylor-series expansions of the propagators and vertices are suppressed by fractional powers of a. That is, the linear approximation holds, and we can approximate the propagators and vertices in the integrand by the continuumlike expressions corresponding to the various linear regions. Hence, for the ith linear region, we substitute in the lattice propagators

$$\nabla_\mu(k) \approx c_{i\mu}\gamma_\mu(k_\mu - \bar{k}_{i\mu}) , \tag{3.12a}$$

where

$$c_{i\mu} = D'_\mu(k)|_{k=\bar{k}_i} \tag{3.12b}$$

is the slope of $D_\mu(k)$ at its zero, $\bar{k}_i$, in the ith linear region. The $c_{i\mu}$'s for the naive, Wilson, and Kogut-Susskind derivatives are displayed in Table I. The continuumlike integrals that result from this linearization are UV convergent, so we can extend the range of integration to $\pm\infty$, making an error that vanishes in the limit $a \to 0$. Then, for the linear region near $k_\mu = 0$ the contribution is exactly equal to the continuum contribution. Thus, it vanishes by virtue of the constraints imposed by the vector and axial-vector Ward identities as given in Eqs. (2.11a) and (2.11b). For the naive derivative, there are additional linear regions that contribute when a component of the loop momentum, say k_μ, is near $\pm\pi/a$. These yield expressions that are equal to the continuum one, except that γ_μ is replaced by $-\gamma_\mu$ in the propagators and vertices. Since any nonzero trace involves an even number of γ_0's and γ_1's, the minus signs always pair up, and the integrand is equal to the continuum one. Again, we can extend the range of integration to $\pm\infty$ with negligible error. The conclusion is that the contributions from these additional linear regions are also equal to the continuum contribution; that is, they also vanish.

TABLE I. The slopes $c_{i\mu}$ of the "naive" derivative function $D^N_\mu(k)$ at its various zeros $\bar{k}_i a$. The first row, corresponding to $\bar{k}_i a = (0,0)$, also gives the slope at the zero of the Wilson derivative function $D^W_\mu(k)$ or the Kogut-Susskind derivative function $D^{KS}_\mu(k)$.

$\bar{k}_i a = (\bar{k}_{i0}, \bar{k}_{i1})a$	c_{i0}	c_{i1}
$(0,0)$	1	1
$(0,\pi)$	1	-1
$(\pi,0)$	-1	1
(π,π)	-1	-1

Note that we could not have reached the conclusion that the higher-order loops give a vanishing contribution without first linearizing the Feynman integrals. Although the exact lattice expressions satisfy the vector and axial-vector Ward identities, the explicit momentum-dependent mass terms in the Wilson and Kogut-Susskind formulations break the chiral invariance, so that Eq. (2.8b) does not become valid until we take the limit $a \to 0$. That is, chiral symmetry is restored for the UV finite graphs, but only in the continuum limit. Furthermore, the connection between the vector and axial-vector vertices [Eq. (2.10)] holds only for the linearized vertices.

Next let us discuss the case (still for $N>2$) in which some of the external photons attach to the fermion loop through seagull vertices. The seagull graphs have no analog in the continuum theory. They are a part of the lattice scheme for regulating the continuum-type graphs. Since the continuum graphs are absolutely convergent for $N>2$, they require no regulator, and we expect the corresponding seagulls to vanish in the limit $a \to 0$. We can demonstrate this vanishing of the seagulls by an explicit power-counting argument. A loop to which N photons are connected by M vertices (some of which are seagulls) contains M fermion propagators. Note that $N \geq M$. From Eqs. (3.6) and (3.8), it is easy to see that the maximum magnitude of a $V^{(i)}$ vertex is a^{i-1}. Replacing each of the vertices by its maximum magnitude, we obtain a factor a^{N-M}. Thus, if a loop involving seagulls is to contribute in the limit $a \to 0$, the following condition must be satisfied:

$$\frac{a^{N-2}}{[a\nabla(k)]^M} \gtrsim 1 . \tag{3.13}$$

This condition can be satisfied only in the linear regions. In fact, the seagull graphs do not contribute even in the

linear regions as $a \to 0$. In Eq. (3.13) we have overestimated the range of integration. We can obtain a better estimate of the integral by retaining the upper bounds for the vertices and using Eq. (3.12) to approximate the propagators with the continuumlike expressions that are valid in the linear regions. This linearization of the propagators is justified by the condition Eq. (3.13). An upper bound on the order of magnitude of the seagull loop integral is then given by

$$\int_{\sim l}^{\sim 1/a} \frac{d^2k}{k^M} a^{N-M} \sim \begin{cases} \left[\frac{1}{a}\right]^{2-N} & \text{from the upper limit ,} \\ l^{2-M} a^{N-M} & \text{from the lower limit .} \end{cases} \tag{3.14}$$

From the RHS of Eq. (3.14), we conclude that for $N>2$ the seagull graphs are negligible.

So far we have considered fermion loops with attached *external* photons. The conclusions are unchanged if one considers photons that are part of some internal momentum loop. This is a consequence of the fact that, in the continuum theory in two dimensions, any loop containing a photon is UV convergent. Thus, in the lattice theory in the limit $a \to 0$, the integral for such a loop contributes only in the linear regions. This conclusion can easily be verified by power-counting arguments of the sort given above. (The exceptional case of a photon that begins and ends at the same seagull vertex leads to a contribution that vanishes in the continuum limit.) Since the lattice photon propagator has only one linear region, i.e., the one near $k=0$, the momentum flowing through the photon is never $O(1/a)$. Consequently, in analyzing the fermion loops, we may regard the photon as having a fixed momentum.

2. *Vacuum polarization*

Now let us consider the case of a fermion loop with two attached photon lines. (Per our preceding argument, these photons can be considered to be external or to be a part of some other graphical loop.) The relevant lattice graphs are shown in Fig. 13. We denote the amplitude associated

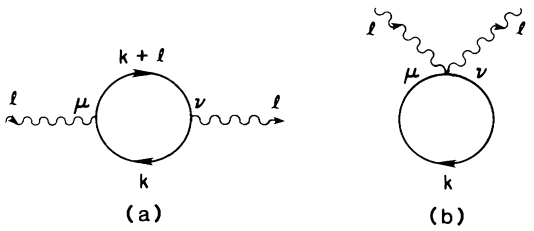

FIG. 13. The Feynman graphs that give the vacuum-polarization contribution in the lattice Schwinger model, (a) the nonseagull graph, (b) the seagull graph.

with the sum of these vacuum-polarization graphs by $\Pi_{\mu\nu}$. As we discussed in Sec. II, in the continuum theory, fermion loops with two photon attachments are superficially logarithmically divergent; they are well defined only after application of a UV regulator. Thus, we expect that the lattice regulator will play a crucial role in this case. Indeed, the power-counting expressions developed in Sec. III B 1 indicate that the case $N=2$ is special, in that the loop integrals receive contributions from k_μ in the entire range from $-\pi/a$ to π/a. Thus, we cannot justify a linearization of the lattice propagators and vertices about the propagator poles. That is, a simple expansion in the explicit powers of a would not be valid.

The continuum expressions for the vacuum-polarization amplitudes are, of course, much simpler than the corresponding lattice expressions. We would like to take advantage of this simplicity by manipulating the lattice expressions so as to obtain quantities for which we can approximate lattice propagators and vertices by their linearized forms. The essential trick is to render the linearized integral UV convergent by subtracting from $\Pi_{\mu\nu}(l)$ its value at zero external momentum $\Pi_{\mu\nu}(0)$. As we shall see, a consequence of the gauge-invariant form of the vertices is that $\Pi_{\mu\nu}(0)=0$. Thus, the subtraction does not affect the value of $\Pi_{\mu\nu}(l)$.

Let us now demonstrate the vanishing of $\Pi_{\mu\nu}(0)$. The expression for the vacuum polarization in terms of generic lattice propagators and vertices is

$$\Pi_{\mu\nu}(l) = -\int_{-\pi/a}^{\pi/a} \frac{d^2k}{(2\pi)^2} \mathrm{Tr}\left[\frac{1}{\sum_\sigma \nabla_\sigma(k+l)+m} V_\mu^{(1)}(k,l) \frac{1}{\sum_\sigma \nabla_\sigma(k)+m} V_\nu^{(1)}(k+l,-l) + \frac{1}{\sum_\sigma \nabla_\sigma(k)+m} V_{\mu\nu}^{(2)}(k,l,-l) \right], \tag{3.15}$$

where the first term in large parentheses comes from the graph of Fig. 13(a) and the second term from the graph of Fig. 13(b). From Eq. (3.8) we immediately obtain the expressions for the vertices at zero photon momentum:

$$V_\mu^{(1)}(p,0) = -e\nabla'_\mu(p) , \tag{3.16a}$$

$$V_{\mu\nu}^{(2)}(p,0,0) = -e^2\delta_{\mu\nu}\nabla''_\mu(p) , \tag{3.16b}$$

$$V_{\mu_1\mu_2\cdots\mu_n}^{(n)}(p,0,\ldots,0) = -e^n\delta_{\mu_1\mu_2}\delta_{\mu_1\mu_3}\cdots\delta_{\mu_1\mu_n}\nabla_{\mu_1}^{(n)}(p) , \tag{3.16c}$$

where the primes indicate differentiation with respect to p. The form of Eqs. (3.16) is a consequence of the gauge invariance of the theory. Using Eqs. (3.16), we see that the vacuum polarization at zero external momentum is

$$\Pi_{\mu\nu}(0)=-e^2\int_{-\pi/a}^{\pi/a}\frac{d^2k}{(2\pi)^2}\mathrm{Tr}\left[\frac{1}{\sum_\sigma\nabla_\sigma(k)+\delta}\nabla'_\mu(k)\frac{1}{\sum_\sigma\nabla_\sigma(k)+\delta}\nabla'_\nu(k)+\frac{1}{\sum_\sigma\nabla_\sigma(k)+\delta}\delta_{\mu\nu}\nabla''_\mu(k)\right], \tag{3.17}$$

where, in order to protect $\Pi_{\mu\nu}(0)$ from IR divergences, we have retained a fermion mass δ in the propagators. The fermion mass δ in $\Pi_{\mu\nu}(0)$ plays the role of a regulator mass and is distinct from the fermion mass m in $\Pi_{\mu\nu}(l)$, which we set equal to zero in the Schwinger model. Next we make use of a well-known identity for the total derivative of a fermion propagator:

$$\frac{d}{dk_\mu}\frac{1}{\sum_\sigma\nabla_\sigma(k)+\delta}=\frac{1}{\sum_\sigma\nabla_\sigma(k)+\delta}\nabla'_\mu(k)\frac{1}{\sum_\sigma\nabla_\sigma(k)+\delta}\ . \tag{3.18}$$

Inserting Eq. (3.18) into Eq. (3.17), we see that the integrand for the vacuum polarization at zero momentum is a perfect derivative:

$$\Pi_{\mu\nu}(0)=-e^2\int_{-\pi/a}^{\pi/a}\frac{d^2k}{(2\pi)^2}\frac{d}{dk_\mu}\mathrm{Tr}\left[\frac{1}{\sum_\sigma\nabla_\sigma(k)+\delta}\nabla'_\nu(k)\right]. \tag{3.19}$$

Since $\nabla_\sigma(k)$ is a periodic function of k_μ with period $2\pi/a$, the surface terms in the k_μ integral cancel. Thus, we reach the conclusion that $\Pi_{\mu\nu}(0)$ vanishes.

Now we can discuss the power counting for the vacuum polarization. For the unsubtracted expression $\Pi_{\mu\nu}(l)$, the power-counting condition that determines whether the graphs contribute can be obtained by substituting $N=2$ in Eqs. (3.11a) and (3.13). The result is

$$\frac{1}{[a\nabla(k)]^2}\gtrsim 1 \tag{3.20a}$$

for the graphs with no seagull vertices and

$$\frac{1}{a\nabla(k)}\gtrsim 1 \tag{3.20b}$$

for the seagull graph. Clearly the conditions of Eqs. (3.20) are satisfied for k outside the linear regions. However, as we shall now demonstrate, the subtraction $\Pi_{\mu\nu}(0)$ improves the convergence of the loop integral by removing the first term in the double Taylor expansion of $\Pi_{\mu\nu}(l)$ in powers of l and m. (The expansion with respect to m arises because the IR regulator mass δ that appears in the subtraction term is different from m. Eventually we set $m=0$; we shall see that our results are independent of δ.) After we make the subtraction, the leading term in the expression is the derivative of the original loop integral with respect to l or m. Therefore, there are contributions that arise from differentiating a vertex or differentiating a propagator. As can be seen from Eqs. (3.16), the derivative of a $V^{(i)}$ vertex is a $V^{(i+1)}$ vertex and the derivative of a propagator is the square of the propagator times either a $V^{(1)}$ vertex or -1, depending on whether the differentiation is with respect to l or m. Then, replacing all quantities except $\nabla(k)$ by the upper bounds on their orders of magnitude, we obtain the following conditions that must be satisfied if the subtracted vacuum polarization is to contribute in the continuum limit:

$$\frac{a}{[a\nabla(k)]^{(2;3)}}\gtrsim 1 \tag{3.21a}$$

for the nonseagull graph and

$$\frac{a}{[a\nabla(k)]^{(1;2)}}\gtrsim 1 \tag{3.21b}$$

for the seagull graph, where the first set of exponents corresponds to the terms that come from differentiating the vertex factors and the second set of exponents corresponds to the terms that come from differentiating the propagator factors. The conditions of Eq. (3.21) are satisfied only if k is in one of the linear regions. Consequently, as in the case of the higher-order graphs, we can obtain a k-independent bound on the order of magnitude of the seagull graph by using Eq. (3.12) to linearize the propagators and restoring the integration over the loop momentum. The resulting upper bound on the order of magnitude of the seagull graph is

$$\int_{\sim l}^{\sim 1/a}\frac{d^2k}{k^{(1;2)}}a^{(2;1)}, \tag{3.22}$$

which is negligible.

Now it is a simple matter to work out the nonseagull contribution to $\Pi_{\mu\nu}(l)-\Pi_{\mu\nu}(0)$ that comes from the linear regions by taking the linearized approximations for the lattice propagators and vertices. The linearized vertices may be computed easily by substituting the linearized lattice derivative of Eq. (3.12) into Eq. (3.16a). We obtain the following expression for the naive, Wilson, and Kogut-Susskind cases:

$$\begin{aligned}\Pi_{\mu\nu}(l)&=\Pi_{\mu\nu}(l)-\Pi_{\mu\nu}(0)\\&=-\sum_i e^2N_f\int\frac{d^2k}{(2\pi)^2}\mathrm{Tr}\left[\frac{1}{\sum_\sigma c_{i\sigma}\gamma_\sigma(k+l)_\sigma+m}c_{i\mu}\gamma_\mu\frac{1}{\sum_\sigma c_{i\sigma}\gamma_\sigma k_\sigma+m}c_{i\nu}\gamma_\nu\right.\\&\qquad\left.-\frac{1}{\sum_\sigma c_{i\sigma}\gamma_\sigma k_\sigma+\delta}c_{i\mu}\gamma_\mu\frac{1}{\sum_\sigma c_{i\sigma}\gamma_\sigma k_\sigma+\delta}c_{i\nu}\gamma_\nu\right],\end{aligned} \tag{3.23}$$

where N_f is the number of fermion flavors ($N_f=1$ for the Wilson and naive derivatives and $N_f=2$ for the Kogut-Susskind derivative). Next we rescale the variables of integration to obtain

$$\Pi_{\mu\nu}(l)=-\sum_i e^2 N_f \int \frac{d^2k}{(2\pi)^2}\frac{1}{|c_{i0}c_{i1}|}\left[\frac{1}{k+\sum_\sigma c_{i\sigma}\gamma_\sigma l_\sigma+m}c_{i\mu}\gamma_\mu\frac{1}{k+m}c_{i\nu}\gamma_\nu-\frac{1}{k+\delta}c_{i\mu}\gamma_\mu\frac{1}{k+\delta}c_{i\nu}\gamma_\nu\right]. \tag{3.24}$$

We recognize Eq. (3.24) as the Pauli-Villars regulated expression for the vacuum polarization with external momentum $c_{i\mu}l_\mu$ [compare with Eq. (2.13)]. In the second term in large parentheses, the external momenta do not appear, so δ plays the same role as a large Pauli-Villars regulator mass, even though it was originally introduced as an IR regulator. We can easily work out the expression in Eq. (3.24) by standard techniques; we find that it is independent of δ. Setting $m=0$, we obtain

$$\Pi_{\mu\nu}(l)=N_f\sum_i\frac{-e^2}{\pi}\frac{1}{|c_{i0}c_{i1}|}\left[\delta_{\mu\nu}{c_{i\mu}}^2-\frac{l_\mu l_\nu {c_{i\mu}}^2 {c_{i\nu}}^2}{\sum_\sigma (c_{i\sigma}l_\sigma)^2}\right]. \tag{3.25}$$

Substituting for the $c_{i\mu}$'s and carrying out the sum over linear regions, we obtain an expression that is proportional to the continuum one:

$$\Pi_{\mu\nu}(l)=N_\pi\left[-\frac{e^2}{\pi}\left[\delta_{\mu\nu}-\frac{l_\mu l_\nu}{l^2}\right]\right], \tag{3.26}$$

where

$$N_\Pi^W=1,\quad N_\Pi^{\mathrm{KS}}=2,\quad \text{and } N_\Pi^N=4,$$

and the quantity in square brackets is just the Euclidean continuum result. In the Wilson and Kogut-Susskind cases, only the linear region near $k=(0,0)$ contributes; in the Wilson case one obtains the continuum result, while in the Kogut-Susskind case an extra factor of 2 arises from N_f. In the naive case, the four linear regions each give a contribution equal to the continuum one. The minus signs from the $c_{i\mu}$'s always pair up because in Eq. (3.23) each $c_{i\mu}$ is associated with a γ_μ and any nonzero trace must contain an even number of γ_0's and γ_1's.

C. The anomaly

Now let us discuss the anomaly $\sum_\mu l_\mu A_{\mu\nu}(l)$, where $A_{\mu\nu}(l)$ is the amplitude that arises from the graphs of Fig. 13 with a γ_5 inserted (as usual) to the right of the γ_μ in vertices with index μ. $A_{\mu\nu}(l)$ is easily computed using the techniques of the previous section. Once again we subtract the amplitude at zero external momentum, introducing a regulator fermion mass δ in the subtraction term. The integrand in $A_{\mu\nu}(0)$ is a perfect differential, so $A_{\mu\nu}(0)$ vanishes and the subtraction does not affect the value of the amplitude. For the subtracted amplitude, only the linear regions contribute in the limit $a\to 0$ and we obtain an expression that has the form of the Pauli-Villars regulated result:

$$\begin{aligned}A_{\mu\nu}(l)&=A_{\mu\nu}(l)-A_{\mu\nu}(0)\\&=-\sum_i e^2 N_f\int\frac{d^2k}{(2\pi)^2}\mathrm{Tr}\left[\frac{1}{\sum_\sigma c_{i\sigma}\gamma_\sigma(k+l)_\sigma+m}c_{i\mu}\gamma_\mu\gamma_5\frac{1}{\sum_\sigma c_{i\sigma}\gamma_\sigma k_\sigma+m}c_{i\nu}\gamma_\nu\right.\\&\qquad\left.-\frac{1}{\sum_\sigma c_{i\sigma}\gamma_\sigma k_\sigma+\delta}c_{i\mu}\gamma_\mu\gamma_5\frac{1}{\sum_\sigma c_{i\sigma}\gamma_\sigma k_\sigma+\delta}c_{i\mu}\gamma_\nu\right].\end{aligned} \tag{3.27}$$

This can be evaluated by standard techniques and yields

$$A_{\mu\nu}(l)=N_f\sum_i\frac{e^2}{\pi}\frac{c_{i0}c_{i1}}{|c_{i0}c_{i1}|}\left[\epsilon_{\mu\nu}-\frac{\sum_\sigma\epsilon_{\mu\sigma}l_\sigma l_\nu {c_{i\nu}}^2}{\sum_\rho (c_{i\rho}l_\rho)^2}\right]. \tag{3.28}$$

Substituting the values of the $c_{i\mu}$'s and summing over the linear regions, we obtain

$$A_{\mu\nu}=N_A\left[\frac{e^2}{\pi}\left[\epsilon_{\mu\nu}-\frac{\sum_\sigma\epsilon_{\mu\sigma}l_\sigma l_\nu}{l^2}\right]\right], \tag{3.29}$$

where

$$N_A^W=1,\quad N_A^{\mathrm{KS}}=2,\quad \text{and } N_A^N=0,$$

and the quantity in square brackets is the Euclidean continuum expression. In contrast with the vacuum-polarization graph, in the anomaly graph the contributions to the naive derivative expression cancel rather than add. This cancellation occurs because a nonvanishing contribution to the trace must contain an even number of γ_0's and an even number of γ_1's. Then, excluding the factor $\gamma_5=\gamma_0\gamma_1$, we find that the remaining factors in the trace in Eq. (3.27) must contain an odd number of γ_0's and an odd number of γ_1's. Thus the minus signs from the $c_{i\mu}$'s are paired if $\bar{k}_i a=(0,0)$ or (π,π) and unpaired if $\bar{k}_i a=(0,\pi)$ or $(0,\pi)$.

D. Results

Having evaluated $\Pi_{\mu\nu}(l)$ and established that the higher-order fermion loops vanish, it is a simple matter for us to compute the mass gap and $\langle\bar{\psi}\psi\rangle$. The mass

gaps can be obtained from Eq. (2.17). The chiral-symmetry order parameters can be obtained from Eq. (2.28). These results along with our results for the anomaly graph are shown in the first three rows of Table II, where all numbers are relative to the continuum result.

TABLE II. The values of $\Pi_{\mu\nu}$, the mass gap, the anomaly, and the chiral order parameter $\langle\bar{\psi}\psi\rangle$ obtained from the continuum limits of the various lattice versions of the Schwinger model. The numbers presented are the values relative to the continuum results.

Derivative	$\Pi_{\mu\nu}$	Mass gap	Anomaly	$\langle\bar{\psi}\psi\rangle$
Wilson	1	1	1	1
Naive	4	2	0	0
Kogut-Susskind	2	$\sqrt{2}$	2	0
DWY	2	$\sqrt{2}$	0	0

IV. THE DWY DERIVATIVE

Now we wish to apply the techniques developed in Sec. III to the lattice Lagrangian based on the DWY derivative. A necessary condition for the applicability of these techniques is that the lattice derivative be a smooth function in momentum space—that is, it must have a Taylor-series expansion. Clearly, this is not the case for the DWY derivative. However, Rabin[10] pointed out that one can perform a partial resummation of perturbation theory to obtain an effective lattice derivative that *does* have a Taylor-series expansion (at least for finite lattice space a). Our strategy, then, will be to apply the methods of Sec. III to the resummed theory.

A. Propagator and vertices

The fermionic part of the DWY action is[7]

$$I^{\mathrm{DWY}}=-a^4\sum_{x,y,\mu}\bar{\psi}(x)\frac{1}{i}\gamma_\mu\tilde{D}_\mu(x-y)\psi(x) -a^2\sum_x m\bar{\psi}(x)\psi(x)\ , \tag{4.1a}$$

where $\tilde{D}_\mu(x)$ is the DWY derivative operator:

$$\tilde{D}_\mu(x)=\int_{-\pi/a}^{\pi/a}\frac{d^2k}{(2\pi)^2}ik_\mu e^{ik\cdot x} =\begin{cases}\dfrac{(-1)^{(x_\mu/a)}}{a^2x_\mu} & \text{if only the } \mu\text{th component of } x \text{ is nonzero}\ ,\\ 0 \ \text{otherwise}\ .\end{cases} \tag{4.1b}$$

The corresponding Feynman-Dirac propagator is

$$S_F^{\mathrm{DWY}}(p)=\left[\sum_\mu\nabla_\mu^{\mathrm{DWY}}(p)+m\right]^{-1} =\left[\sum_\mu\gamma_\mu D_\mu^{\mathrm{DWY}}(p)+m\right]^{-1}, \tag{4.2a}$$

where

$$D_\mu^{\mathrm{DWY}}(p)=p_\mu \quad \text{for } -\pi/a\le p_\mu\le\pi/a \tag{4.2b}$$

and is a periodic function of p with period $2\pi/a$. Interactions with the photon field can be introduced in a gauge-invariant manner by making the minimal substitution

$$\psi(y)\to\psi(y)\exp\left[iea\sum_{w=x}^{y}A_\mu(w)\right] \tag{4.3}$$

in Eq. (4.1a). Expansion of the Lagrangian in powers of the coupling e leads to the Feynman rules for the vertices that are given by Eq. (3.8). These vertices satisfy the usual graphical Ward identities shown in Fig. 11 and, as we have noted previously, can be derived from them. The axial-vector vertices that one obtains by making the substitution

$$\gamma_\mu\to\gamma_\mu\gamma_5$$

satisfy the graphical Ward identities shown in Fig. 12.

B. Rabin's procedure

The essential point of Rabin's resummation procedure is that an expansion of the DWY Lagrangian in powers of

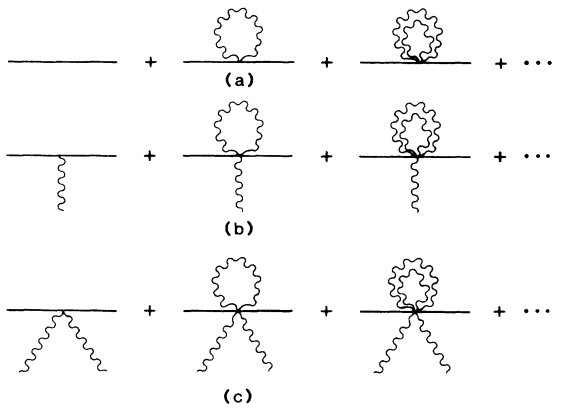

FIG. 14. Tadpole series for (a) the fermion propagator, (b) the fermion—one-photon vertex, and (c) the fermion—two-photon vertex.

the coupling constant e leads to spurious infrared singularities. These singularities manifest themselves through discontinuities in the perturbative propagators and vertices. Such singularities in momentum space, of course, correspond to long-range interactions in coordinate space. Rabin suggests that by summing to all orders in e certain graphs, called the "tadpole" graphs, one can eliminate these spurious singularities. There is a set of tadpole graphs associated with each basic vertex or with the propagator, which consists of the basic vertex or propagator and all graphs obtained by attaching both ends of one or more photons to the vertex or to a common point on the propagator. (See Fig. 14.) Rabin finds that the effect of summing over such a set is to make the following replacement in the basic vertex or propagator:

$$\tilde{D}_\mu(x) \rightarrow \tilde{D}_\mu(x)\tilde{\mathscr{S}}_\mu(x) \equiv \tilde{\mathscr{D}}_\mu(x) , \tag{4.4a}$$

where

$$\tilde{\mathscr{S}}_\mu(x) = \exp\left[-\frac{1}{2}e^2 \int_{-\pi/a}^{\pi/a} \frac{d^2k}{(2\pi)^2} \left| \frac{e^{ik_\mu x_\mu} - 1}{d_\mu(k)} \right|^2 K_{\mu\mu}(k) \right] . \tag{4.4b}$$

Here we have made a slight generalization of Rabin's procedure by using the *complete* photon propagator $K_{\mu\nu}$ in constructing the sets of resummed graphs and, consequently, in Eq. (4.4). We call the function $\tilde{\mathscr{S}}_\mu(x)$ the "smearing function." It has the effect of making the DWY derivative sufficiently local in coordinate space so that it is "smeared" into a smooth function in momentum space.

Although we need the complete photon propagator in order to compute $\tilde{\mathscr{S}}_\mu(x)$, we do not know it until we have solved the theory. However, we can arrive at an ansatz for the complete lattice photon propagator by requiring that it take the form of the continuum propagator in the limit $a \rightarrow 0$:

$$K_{\mu\nu}(k) = \frac{1}{\sum_\sigma d_\sigma^2(k) + \mu^2} \left[\delta_{\mu\nu} - \frac{d_\mu(k) d_\nu(k)}{\sum_\sigma d_\sigma^2(k)} \right] \underset{a\rightarrow 0}{\rightarrow} \frac{1}{k^2+\mu^2} \left[\delta_{\mu\nu} - \frac{k_\mu k_\nu}{k^2} \right] . \tag{4.5}$$

Here we have taken the ansatz that is appropriate to Landau gauge. It turns out that only the behavior of the complete propagator in the limit $a \rightarrow 0$ is relevant to the computation of $\tilde{\mathscr{S}}_\mu(x)$. We can display the a dependence in $\tilde{\mathscr{S}}_\mu(x)$ explicitly by rewriting Eq. (4.4) in terms of the dimensionless variables

$$\kappa_\mu = k_\mu a \quad \text{and} \quad n_\mu = x_\mu / a \tag{4.6}$$

to obtain

$$\tilde{\mathscr{S}}_\mu(x) = \exp\left[-\frac{1}{2}e^2 \int_{-\pi}^{\pi} \frac{d^2\kappa}{(2\pi^2)} (\tfrac{1}{4}a^2) \frac{\sin^2 \frac{1}{2}\kappa_\mu n_\mu}{\sin^2 \frac{1}{2}\kappa_\mu} \frac{1}{\sum_\sigma \sin^2 \frac{1}{2}\kappa_\sigma + \frac{1}{4}\mu^2 a^2} \left[1 - \frac{\sin^2 \kappa_\mu}{\sum_\sigma \sin^2 \kappa_\sigma} \right] \right] . \tag{4.7}$$

We need the leading behavior of $\tilde{\mathscr{S}}_\mu(x)$ in the limit $a \rightarrow 0$. This comes from the region of integration in which the photon propagator is peaked: namely,

$$|\kappa| \sim \mu a .$$

In this region, we can approximate the integrand factors by the linear terms in their Taylor-series expansions to obtain

$$\tilde{\mathscr{S}}_\mu(x) \underset{a\rightarrow 0}{\rightarrow} \exp\left[-\frac{1}{2}e^2 \int_{-\pi}^{\pi} \frac{d^2\kappa}{(2\pi)^2} a^2 n_\mu^2 \frac{1}{\kappa^2 + \mu^2 a^2} \left[1 - \frac{\kappa_\mu^2}{\kappa^2} \right] \right] \tag{4.8a}$$

$$\underset{a\rightarrow 0}{\rightarrow} \exp[(-e^2/8\pi)(a n_\mu)^2 \ln(1/\mu a)] . \tag{4.8b}$$

Here we have dropped some constant terms in the exponent, which affect only the normalization of $\tilde{\mathscr{S}}_\mu(x)$. As can be seen from Eqs. (4.4a) and (4.8), $\tilde{\mathscr{S}}_\mu(x)$ makes $\tilde{D}_\mu(x)$ local by providing a Gaussian damping.

In order to work out the diagrammatic solution of the Schwinger model, we need the Fourier transform of the smeared derivative

$$\mathscr{D}_\mu(p) = \sum_{n_\mu} a e^{ip_\mu x_\mu} \tilde{\mathscr{D}}_\mu(x) . \tag{4.9}$$

This is given by the convolution

$$\mathscr{D}_\mu(p) = \int_{-\pi/a}^{\pi/a} \frac{dp'_\mu}{2\pi} \mathscr{D}_\mu(p - p') \mathscr{S}_\mu(p') , \tag{4.10a}$$

where

$$\mathscr{S}_\mu(p')=\sum_{n_\mu} a e^{ip'_\mu x_\mu}\tilde{\mathscr{S}}_\mu(x)\ . \tag{4.10b}$$

In the limit $a\to 0$, we can replace $\tilde{\mathscr{S}}_\mu(x)$ in Eq. (4.10b) by the expression (4.8b). Then, the sum in Eq. (4.10) can be approximated by an integral:

$$\mathscr{S}_\mu(p') \underset{a\to 0}{\to} \int dx_\mu e^{ip'_\mu x_\mu}\exp[-(e^2/8\pi)\ln(1/\mu a)x_\mu{}^2]=\left[\frac{8\pi^2}{e^2\ln(1/\mu a)}\right]^{1/2}\exp\left[\frac{2\pi}{e^2\ln(1/\mu a)}p'^2_\mu\right]\ . \tag{4.11}$$

Thus, in the convolution Eq. (4.10a), the DWY derivative is "smeared" by a Gaussian of width

$$\sigma=e\ln^{1/2}(1/\mu a)/(2\sqrt{\pi})\ .$$

The width of the smearing function $\mathscr{S}_\mu(p)$ grows as $a\to 0$, but not as fast as the Brillouin zone, which grows like $1/a$. The effect of the smearing on the DWY derivative is shown in Fig. 15. As can be seen, the smearing smooths the singularity at $p_\mu=\pm\pi/a$. It is easy to verify that the Gaussian smearing function guarantees that $\mathscr{D}_\mu(p)$ posseses a Taylor-series expansion about $p_\mu=\pi/a$. Note, however, that the slope of $\mathscr{D}_\mu(p)$ at $p_\mu=\pi/a$ tends to infinity in the limit $a\to 0$. As we shall see, this feature of the smeared DWY derivative necessitates a slightly more sophisticated treatment of the continuum limit than the one given in Sec. III. For future reference, we compute the slope of $\mathscr{D}_\mu(p)$ explicitly. This is easily accomplished by differentiating Eq. (4.10a) with respect to p_μ:

$$\mathscr{D}'_\mu(p)=\frac{\partial}{\partial p_\mu}\mathscr{D}_\mu(p)=1-\frac{1}{a}\mathscr{S}_\mu(\,|p_\mu|-\pi/a)\ . \tag{4.12}$$

The leading values in the limit $a\to 0$ of the slopes at $p_\mu=0$ and $p_\mu=\pi/a$ are given in Table III.

C. The Schwinger model

Now let us work out the power counting for the various Schwinger model graphs for the DWY derivative. We will make the arguments along the lines of Sec. III. However, in the case of the smeared DWY derivative, an additional refinement is necessary. Because the slope of the $\mathscr{D}_\mu(p)$ at $p_\mu=\pi/a$ tends to infinity as $a\to 0$, it is important to treat the zero of $\mathscr{D}_\mu(p)$ at $p_\mu=\pi/a$ separately from the zero at $p_\mu=0$. To this end, we split the Brillouin zone into two regions: region I, the region that includes $p_\mu=0$ and extends to within $O(e\ln^{1/2}(1/\mu a))$ of $p_\mu=\pm\pi/a$; region II, the region within $O(e\ln^{1/2}(1/\mu a))$ of $p_\mu=\pm\pi/a$. These regions of the Brillouin zone are shown in Fig. 15. Note that in Region I the characteristic momentum scale of the DWY derivative function is $1/a$, whereas in Region II it is $e\ln^{1/2}(1/\mu a)$. That is, in Region I the DWY derivative function varies significantly only for momentum changes of $O(1/a)$, but in Region II it varies significantly for momentum changes of $O(e\ln^{1/2}(1/\mu a))$. Given this demarcation of the Brillouin zone, there are four possibilities to consider with regard to a graphical loop momentum k: (i) k_0 and k_1 in Region I; (ii) k_0 in Region I and k_1 in Region II; (iii) k_0 in Region II and k_1 in Region I; (iv) k_0 in Region II and k_1 in Region II.

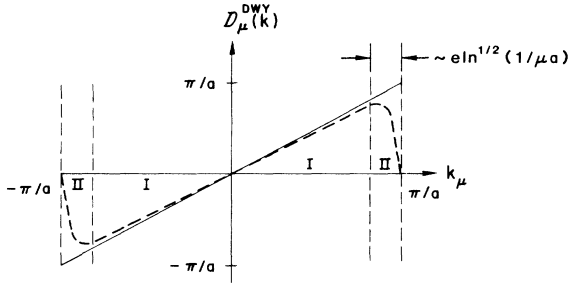

FIG. 15. The "smeared" DWY derivative function in momentum space. The numerals I and II indicate regions of the Brillouin zone, as discussed in the text.

1. Higher-order loops

In this subsection we analyze the contributions involving a fermion loop with N attached photons for the case $N>2$. Our aim is to show that these contributions vanish in the continuum limit. The analysis follows essentially along the lines of the procedure given in Sec. III. However, for the smeared DWY derivative, it turns out that the power-counting arguments are dependent on the choice of Lorentz components of the amplitude. Our strategy is to use the constraints imposed by the vector Ward identity of Fig. 11 to express some of the Lorentz components of the amplitude in terms of other Lorentz components that are more convenient to analyze. Suppose that an attached photon is external and carries momentum l_1 and Lorentz index μ_1. If one sums over all connections of that photon to the loop, including seagull connections, then the vector Ward identity leads to the constraint of Eq. (2.8a), which

TABLE III. The slopes $c_{i\mu}$ of the DWY derivative function $D_\mu^{\rm DWY}(k)$ at its various zeros $\bar{k}_i a$.

$\bar{k}a=(\bar{k}_0,\bar{k}_1)a$	c_{i0}	c_{i1}
$(0,0)$	1	1
$(0,\pi)$	1	$\dfrac{-\sqrt{8}\pi}{ea\ln^{1/2}(1/\mu a)}$
$(\pi,0)$	$\dfrac{-\sqrt{8}\pi}{ea\ln^{1/2}(1/\mu a)}$	1
(π,π)	$\dfrac{-\sqrt{8}\pi}{ea\ln^{1/2}(1/\mu a)}$	$\dfrac{-\sqrt{8}\pi}{ea\ln^{1/2}(1/\mu a)}$

relates the components with Lorentz index $\mu_1=0$ to the components with Lorentz index $\mu_1=1$. For an *internal* photon, the Rabin resummation procedure complicates this analysis. We defer the discussion of that case until the end of the subsection. For reasons that will become apparent later, it is most convenient to carry out the analysis for the components of the loop amplitude in which one of the Lorentz indices is 0 and another of the indices is 1. For the moment, we leave all the other indices unspecified.

We now exhibit the power counting for the loops with N external photons for $N>2$. We treat the seagull and nonseagull graphs together. As usual, each of the fermion propagators contributes a factor whose magnitude is given by Eq. (3.9). Each of the vertices supplies a factor $V^{(i)}$. Substituting $\mathscr{D}_\mu(p)$ into Eqs. (3.8), we obtain the following upper bounds for the orders of magnitude of the vertices:

$$|V_\mu^{(i)}\ldots(k,\ldots)| \sim \begin{cases} a^{i-1} & \text{for } k_\mu \text{ in region I}, \\ \dfrac{1}{a}\left[\dfrac{1}{e\ln^{1/2}(1/\mu a)}\right]^i & \text{for } k_\mu \text{ in region II}. \end{cases} \tag{4.13}$$

One can arrive at the orders of magnitude in Eq. (4.13) by considering either the characteristic momentum scales of $\mathscr{D}_\mu(p)$ in each region or, more explicitly, by making use of Eq. (4.12) and its derivatives. [As can be seen from Eq. (4.12), for $i>1$ the leading power of a in $V_\mu^{(1)}$ actually vanishes in region I.] In the loop graph, the order of magnitude of the factor that comes from the vertices depends on the values of the Lorentz indices that remain unspecified. In order to obtain an upper bound on the vertex factor, we shall suppose that these unspecified indices take on the values that give the largest orders of magnitude. From Eq. (4.13) we see that this occurs if the Lorentz index of the vertex is the same as the Lorentz index of a component of the loop momentum that is in region II. Thus, we arrive at the following assignments of indices: in case (ii) we take all of the unspecified Lorentz indices in the loop vertices to be 1 and all of the seagulls' Lorentz indices to be 1; in case (iii) we take the opposite assignment of indices. Then, the upper bounds on the orders of magnitude of the factor from the loop vertices are

$$\begin{aligned} &a^{N-M} \text{ for case (i)}, \\ &\left[\frac{1}{ae\ln^{1/2}(1/\mu a)}\right]^{N-1} a^{N-M} \text{ for cases (ii) and (iii)}, \\ &\left[\frac{1}{ae\ln^{1/2}(1/\mu a)}\right]^{N} a^{N-M} \text{ for case (iv)}, \end{aligned} \tag{4.14}$$

where we are using our previous notation that M is the number of vertices. The range of integration is $O(1/a)$ in region I and $O(e\ln^{1/2}(1/\mu a))$ in region II. Thus, we find the following conditions that must be satisfied if the loop amplitudes are to contribute in the continuum limit:

$$\begin{aligned} &\frac{a^{N-2}}{[a\nabla(k)]^M} \gtrsim 1 \text{ for case (i)}, \\ &\left[\frac{1}{e\ln^{1/2}(1/\mu a)}\right]^{N-2} \frac{1}{[a\nabla(k)]^M} \gtrsim 1 \text{ for cases (ii)—(iv)}. \end{aligned} \tag{4.15}$$

The conditions of Eq. (4.15) imply that $a\nabla(k)$ vanishes as $a\to 0$. In case (i), $a\nabla(k)$ vanishes like a fractional power of a: namely, $a^{(N-2)/M}$; in cases (ii)—(iv), $a\nabla(k)$ vanishes like a fractional power of $1/e\ln^{1/2}(1/\mu a)$: namely,

$$[1/e\ln^{1/2}(1/\mu a)]^{(N-2)/M}.$$

In either case, $a\nabla(k)$ is much less than ~ 1, which implies that the loop momentum k is in one of the linear regions of the smeared DWY propagator, that is, near $k_\mu=0$ or $k_\mu=\pi/a$. It follows that for case (i) the quadratic and higher-order terms in the Taylor-series expansions for the propagators and vertices are suppressed by fractional powers of a relative to the linear ones. However, for cases (ii)—(iv), the higher-order terms are suppressed only by fractional powers of $1/e\ln^{1/2}(1/\mu a)$ relative to the linear ones. In this respect, the smeared DWY derivative differs from the ones discussed in Sec. III.

Now we can use the linear approximation Eq. (3.12) in the propagators and vertices in the various Feynman integrals that contribute to the loop amplitude. In the DWY case, the $c_{i\mu}$ are given in Table III. The nonseagull graphs give contributions from each linear region whose integrands are proportional to the continuum ones. We can extend the ranges of integration to $\pm\infty$, making an error of $O(a)$ in case (i) and of $O(1/e\ln^{1/2}(1/\mu a))$ in cases (ii)—(iv). The resulting contributions then have the following properties: (1) they satisfy the vector Ward identity (Fig. 11); (2) the expression that one obtains by making the replacement $\gamma_\mu\to\gamma_\mu\gamma_5$ in any of the vertices satisfies the axial-vector Ward identity (Fig. 12); (3) the expressions with γ_5's are related to the one without γ_5's through the completely antisymmetric tensor [see Eq. (2.9)]. Thus, by the arguments of Sec. II, we see that the contribution of the nonseagull amplitude vanishes in the continuum limit. For the seagull graphs, we linearize

only the propagators, replacing the vertices with their upper bounds. Then the upper bounds on the orders of magnitude of the seagull graphs are given by

$$\int_{\sim l}^{\sim 1/a} \frac{d^2k}{k^M} a^{N-M} \quad \text{for case (i)} ,$$

$$\int_{\sim l}^{\sim e \ln^{1/2}(1/\mu a)} \frac{d^2\tilde{k}}{\tilde{k}^M} \left[\frac{1}{e \ln^{1/2}(1/\mu a)} \right]^{N-M} \quad \text{for cases (ii) and (iii)} , \tag{4.16a}$$

$$\int_{\sim l}^{\sim e \ln^{1/2}(1/\mu a)} \frac{d^2k}{k^M} \left[\frac{1}{e \ln^{1/2}(1/\mu a)} \right]^{N-M} \quad \text{for case (iv)} ,$$

where

$$\tilde{k}_\mu = \begin{cases} ae \ln^{1/2}(1/\mu a) k_\mu & \text{for } k_\mu \text{ in region I} , \\ k_\mu & \text{for } k_\mu \text{ in region II} . \end{cases} \tag{4.16b}$$

These expressions are all negligible in the continuum limit for $N > M$ and $N > 2$.

Suppose that we had not specified that at least one of the Lorentz indices in the loop be one and at least one of the Lorentz indices be zero. Then we would have obtained an extra factor of $1/[ae \ln^{1/2}(1/\mu a)]$ on the LHS of Eqs. (4.14) and (4.15) in cases (ii) and (iii). This would make it appear that there could be a contribution from outside the linear region. That is, the explicit factor of $1/a$ in the power counting might lead one to expect that the linearized integrals would exhibit a UV divergence. However, the vector Ward identity fixes the value of the apparently divergent Lorentz components of the loop in terms of the Lorentz components that we have examined already. Furthermore, it guarantees that the UV divergent pieces of the linearized integrals cancel if one actually carries out an explicit calculation.

Finally, let us discuss the case, still for $N > 2$, in which some of the photons attached to the fermion loop are internal. If a complete photon propagator connects one fermion loop to another, then we may regard the photon momentum as fixed, and our preceding analysis applies. If a complete photon propagator begins and ends on the same fermion loop, then there is a difficulty in using the vector Ward identity in order to constrain the Lorentz components of the amplitude. The problem is that, in any order of perturbation theory, some of the seagull graphs that are required for gauge invariance have already been incorporated into the smeared DWY propagators and vertices through the Rabin resummation procedure. These seagull graphs are the ones in which a complete photon propagator begins and ends at the same seagull vertex. By following the Rabin procedure, we selectively resum this gauge-noninvariant class of graphs, and thereby destroy the manifest gauge invariance at each order in a loop expansion. Thus, vector-current conservation does not hold for every Lorentz index of the fermion-loop amplitude. However, at least two of the Lorentz indices do not involve complete photon propagators that begin and end on the same fermion loop—otherwise we would have a disconnected graph. For these two Lorentz indices, the loop amplitude satisfies vector-current conservation, so we are free to specify these two indices as above. Then, following our preceding arguments, we conclude that all fermion loops with $N > 2$ are negligible in the continuum limit.

2. *Vacuum polarization*

Now we consider the case of a fermion loop with two attached photons (Fig. 13)—the vacuum polarization $\Pi_{\mu\nu}$. As in the previous subsection, we can use vector-current conservation to express all the components of $\Pi_{\mu\nu}$ in terms of just one of the components. Again, we choose to analyze the component that has one Lorentz index with the value 0 and one Lorentz index with the value 1: namely, Π_{01}. This component is chosen because, superficially, it appears to have the most convergent UV behavior. Note that there is no seagull contribution to Π_{01}. Reference to Eq. (4.15) with $N=2$ indicates that the vacuum polarization receives contributions from loop momenta outside the linear region. However, following the procedure of Sec. III B 2, we subtract the vacuum polarization at zero momentum. The subtraction $\Pi_{01}(0)$ removes the first term in the double Taylor expansion of $\Pi_{01}(l)$ in powers of l and m. The leading term in the subtracted expression is obtained by differentiating the original amplitude with respect to the mass m, which we eventually set equal to zero, or with respect to the external momentum l. As explained in Sec. III, the effect of differentiating a $V^{(i)}$ vertex is to replace it with a $V^{(i+1)}$ vertex, and the effect of differentiating a propagator is to square the propagator and to multiply it either by $V^{(1)}$ or by -1, depending on whether the differentiation is with respect to l or m We retain the factor $V^{(1)}$, since it always gives the larger estimate. In cases (ii) and (iii), where the order of magnitude depends on vertex or propagator term that is differentiated, we retain the term that produces the largest order of magnitude. Then, replacing all quantities except $\nabla(k)$ with the upper bounds on their orders of magnitude, we obtain the following conditions that must be satisfied if $\Pi_{01}(l) - \Pi_{01}(0)$ is to contribute in the continuum limit:

$$\begin{aligned} &\frac{a}{[a\nabla(k)]^{(2;3)}} \gtrsim 1 \quad \text{for case (i)} , \\ &\frac{1}{e \ln^{1/2}(1/\mu a)} \frac{1}{[a\nabla(k)]^{(2;3)}} \gtrsim 1 \quad \text{for cases (ii)–(iv)} , \end{aligned} \tag{4.17}$$

where the first set of exponents corresponds to the terms that arise from differentiating the vertices and the second set of exponents corresponds to the terms that arise from differentiating the propagators. The conditions of Eq. (4.17) are satisfied only for k in one of the linear regions of the smeared DWY derivative. Thus, we can approximate the propagators and vertices by the linear term in their Taylor expansions. As can be seen from Eq. (4.17), the quadratic and higher-order terms are suppressed by fractional powers of a in case (i) and by fractional powers of $1/e \ln^{1/2}(1/\mu a)$ in cases (ii)–(iv).

Having justified a linear approximation for the amplitude, we can follow the procedure of Sec. III, making use of Eqs. (3.12), to obtain a linearized expression for Π_{01}.

The values for the other Lorentz components of the vacuum polarization can be inferred from the vector Ward identity. Just as for the lattice derivatives examined in Sec. III, the DWY derivative leads to the result of Eq. (3.25). However, in the DWY case, the $c_{i\mu}$'s are given in Table III.

Next we substitute the $c_{i\mu}$'s into Eq. (3.25) and take the limit $a\to 0$. The linear regions near $k=(0,0)$ and $k=(\pi/a,\pi/a)$ each give a contribution equal to the continuum one; the linear regions near $k=(0,\pi/a)$ and $k=(\pi/a,0)$ do not contribute in the limit $a\to 0$. [For the components Π_{11} and Π_{00}, the linear regions near $k=(0,\pi/a)$ and $k=(\pi/a,0)$, respectively, give divergent contributions to each of the two terms in large parentheses in Eq. (3.25). However, these divergent contributions and the finite remainder cancel between the two terms. The cancellation of the divergent contributions is a consequence of the vector Ward identity, which guarantees that no component of $\Pi_{\mu\nu}$ can have a greater order of magnitude than Π_{01}—even though simple power counting would admit the possibility.] Altogether, we obtain a result that is just twice the continuum one. That is, in Eq. (3.26),

$$N_{\Pi}^{\mathrm{DWY}}=2\ . \tag{4.18}$$

D. The anomaly

Now let us discuss the anomaly for the smeared DWY derivative. As usual, we define $A_{\mu\nu}(l)$ as the amplitude obtained by making the replacement $\gamma_\mu\to\gamma_\mu\gamma_5$ in the vertex of index μ in $\Pi_{\mu\nu}(l)$. The computation of $A_{\mu\nu}(l)$ proceeds exactly as in the case of the vacuum polarization. For the components A_{01} and A_{10}, we subtract the amplitude at zero external momentum. The subtracted amplitude receives contributions only from the linear regions. Taking the linear approximations for propagators and vertices, we obtain explicit expressions for A_{01} and A_{10}. The other components can be inferred from these by using the fact that the index ν of $A_{\mu\nu}$ satisfies vector-current conservation which implies that $l_\nu A_{\mu\nu}(l)=0$. The result is Eq. (3.28), with the $c_{i\mu}$'s given by Table III. Substituting the $c_{i\mu}$'s into Eq. (3.28) and taking the limit $a\to 0$, we obtain

$$A_{\mu\nu}^{\mathrm{DWY}}=\frac{2e^2}{\pi}\left[\epsilon_{\mu\nu}-\frac{\sum_\alpha \epsilon_{\mu\alpha}l_\alpha l_\nu}{l^2}\right]-\frac{2e^2}{\pi}\left[\epsilon_{\mu\nu}-\frac{\sum_\alpha \epsilon_{\mu\alpha}l_\alpha l_\nu}{2l_\nu^2}\right]\ . \tag{4.19}$$

The first term in Eq. (4.19) is twice the continuum result and comes equally from the linear regions near $k=(0,0)$ and $k=(\pi/a,\pi/a)$. The second term is noncovariant and comes from the linear regions near $k=(0,\pi/a)$ and $k=(\pi/a,0)$. The noncovariance arises from the fact that the velocity of light is infinite or infinitesimal in these last two linear regions. Unlike the Wilson and Kogut-Susskind derivatives, the DWY derivative does not yield an $A_{\mu\nu}$ that is proportional to the continuum one. In fact, even though $A_{\mu\nu}$ is nonzero, it is easy to see that the anomaly vanishes:

$$\sum_\mu l_\mu A_{\mu\nu}^{\mathrm{DWY}}(l)=0\ . \tag{4.20}$$

E. Gauge invariance

In the preceding discussion of the Schwinger model with the DWY derivative, we have made a particular choice of gauge: namely, the Landau gauge. Of course we expect the final results to be independent of gauge. Thus, it is worthwhile to discuss the form that our analysis would take for another choice of gauge. Then, in the continuum limit the complete photon propagator would have the form

$$K_{\mu\nu}(l)=\frac{\delta_{\mu\nu}-l_\mu l_\nu/l^2}{l^2+\mu^2}+\alpha\frac{l_\mu l_\nu/l^2}{l^2}\ , \tag{4.21}$$

where α is a parameter that specifies the gauge. In general, there would be a pole at $l^2=0$ in addition to the pole at $l^2=\mu^2$. In the expression for the smearing function Eq. (4.4b), this additional pole would produce a logarithmic infrared divergence. We could regulate this divergence by introducing a photon mass λ, which we would ultimately take to zero (or, equivalently, we could give the lattice a finite spatial extent, which we would ultimately take to infinity). The order of the limits $a\to 0$ and $\lambda\to 0$ would then affect the procedure crucially. If we were to take $a\to 0$ first, then λ would play a role similar to that of μ in the smearing function. The analysis would go through as before. If we were to take $\lambda\to 0$ first, then, in general, higher-order graphs involving photon loops would exhibit spurious infrared divergences involving powers of $e\ln(\lambda a)$. These divergences would overcome the usual suppression due to the fractional powers of a and $1/\ln a$ that accompany the higher-order graphs. As a result, our procedure for solving the model would break down. Presumably, these spurious infrared divergences could be resummed by making use of one of the all-orders procedures for treating the infrared problem in QED (for example, the Grammer-Yennie formalism[20]). This would merely be a cumbersome way to recover the Landau-gauge starting point.

F. Results

Having computed the vacuum polarization and established that the higher-order loops vanish, it is a simple matter for us to compute the mass gap. The geometric series involving $\Pi_{\mu\nu}$ and the Landau-gauge photon propagator is easily summed as in Sec. II. We obtain the complete photon propagator of Eq. (4.5), thus verifying our ansatz. Since $\Pi_{\mu\nu}$ is twice the continuum result, the mass gap μ is $\sqrt{2}$ times the continuum one. By substituting $N_\Pi=2$ into Eq. (2.28), we find that $\langle\bar\psi\psi\rangle$ vanishes. As we have seen, the anomaly vanishes, as expected from the manifest chiral invariance of the DWY Lagrangian. These results are summarized in the last row of Table II.

V. SUMMARY AND DISCUSSION

We now discuss the results that we have obtained from the exact solutions in the continuum limit of the various versions of the lattice Schwinger model. These are summarized in Table II.

As expected, the Wilson derivative reproduces the continuum results. There is no species doubling, so the mass gap takes on the continuum value. The chiral symmetry that appears in the unregulated continuum Lagrangian is broken by the Wilson lattice regularization. This phenomenon is similar to the chiral-symmetry breaking that occurs in the continuum theory when one introduces a gauge-invariant UV regulator. Hence, the anomaly and $\langle\bar{\psi}\psi\rangle$ can acquire nonzero values. The lack of doubling in the continuum limit of the Wilson theory leads to the result that the values they acquire are the continuum ones.

The naive derivative exhibits spectrum doubling, which leads to a quadrupling of the vacuum polarization and a doubling of the mass gap. The naive lattice-regulated Lagrangian contains an explicit chiral symmetry, so we expect the anomaly in the divergence of the axial-vector current to vanish. In fact—owing to the doubling phenomenon—the graph that would lead to the anomaly vanishes identically in the continuum limit. Since it is impossible to break a continuous symmetry spontaneously in two dimensions,[21] the vacuum state in the "naive" theory must be chirally invariant, and, hence, we expect $\langle\bar{\psi}\psi\rangle$ to vanish. This expectation is born out by our calculation. There, the vanishing is a direct consequence of the presence of more than one fermion species, which is, of course, related to the chiral symmetry of the Lagrangian.

In the case of the Kogut-Susskind derivative, there are two explicit flavors in the Lagrangian and no additional doubling occurs in the continuum limit. The two flavors lead to a doubling of the vacuum polarization and the anomaly and increase the mass gap by $\sqrt{2}$. There is a continuous remnant of chiral symmetry under which the Kogut-Susskind Lagrangian, and, hence, the vacuum, must be invariant—namely, rotations in the τ_3 direction in flavor space. Since $\bar{\psi}\psi$ is not invariant under even this remnant of chiral symmetry, it vanishes. At first sight, this result is somewhat surprising, since the anomaly is nonzero in the Kogut-Susskind case. Note, however, that the current corresponding to the remnant of the continuous chiral symmetry is the τ_3 *flavor* axial-vector current, not the U(1) axial-vector current. It is easy to see that this flavor current has a vanishing anomaly.

Finally, let us discuss the DWY Lagrangian version of the lattice Schwinger model. Initially, it was hoped that the DWY formulation would allow one to define a chirally symmetric lattice theory without species doubling. The basic idea was that one could eliminate the extra zeros of the lattice derivative function, and their attendant extra species, by introducing singularities at the Brillouin zone boundaries. Since the original no-go theorems[3,4,6] were predicated on the basis of a smooth derivative function, they did not rule out this possibility.

However, it became apparent, through the work of Karsten and Smit,[11,12] that the singularity in the DWY derivative function leads to pathologies at the one-loop level. Rabin[1] suggested that these problems are artifacts of the perturbation expansion and that they can be overcome through a partial resummation of the perturbation series. We have adopted Rabin's procedure in this work and have found that the Rabin resummation does, indeed, remove the singularities in the DWY derivative function for finite lattice spacing. In the limit $a\to 0$, however, the slope at $p_\mu=\pi/a$ becomes infinite once again. Although the Rabin resummation smooths the singularities in the derivative function, in the process it reintroduces the extra zeros and, thus, the possibility of doubling.

By using Rabin's procedure to reorganize the perturbation series, we were able to obtain the exact solution of the DWY Lagrangian version of the lattice Schwinger model in the continuum limit, to all orders in perturbation theory. We found that extra fermion species *do* contribute. The two species from $p=(0,0)$ and $p=(\pi/a,\pi/a)$ lead to a doubling of the continuum result for the vacuum polarization. The species at $p=(0,\pi/a)$ and $p=(\pi/a,0)$ do not contribute to the vacuum polarization in the continuum limit. Hence, the mass gap is increased by a factor $\sqrt{2}$ relative to the continuum value. In the case of the anomaly graph, all four species contribute. The two at $p=(0,0)$ and $p=(\pi/a,\pi/a)$ just double the continuum result and the two at $p=(0,\pi/a)$ and $p=(\pi/a,0)$ give a contribution that is noncovariant in the continuum limit. The noncovariant contributions correspond to species whose velocities are either infinite or infinitesimal. When one takes the divergence of the axial-vector current, the noncovariant contribution cancels the covariant one. This phenomenon of anomaly cancellation in the DWY lattice Lagrangian theory due to infinite velocity species was noted by Ninomiya and Tan.[5] Our results confirm their conclusions. Of course, the vanishing of the anomaly is no surprise, since axial-vector-current conservation is manifest at each stage of the calculation. Similarly, from the chiral symmetry of the DWY Lagrangian, we expect $\langle\bar{\psi}\psi\rangle$ to vanish. Indeed it does—through the mechanism of doubling of the vacuum polarization.

Based on these results, we conclude that the DWY lattice Lagrangian formulation does not evade the no-go theorem of Ninomiya and Tan. Furthermore, it does not reproduce the continuum Schwinger model and is, therefore, not a satisfactory lattice transcription.

We can understand intuitively the failure of the DWY Lagrangian approach in terms of the constraints imposed by gauge invariance in the interacting theory. In the DWY formulation, one attempts to avoid the problem of species doubling by squeezing the regions surrounding the extra zeros in the lattice derivative function into vanishingly small intervals in the Brillouin zone. The problem with this approach is that gauge invariance requires a corresponding increase in the strength of the vertices describing the interaction of the fermions with the gauge field. As we have seen, the Ward identities dictate that the couplings to the gauge field grow like the slope of the derivative function. Consequently, one cannot neglect the contributions from the extra zero crossings, even if these zero crossings are discontinuous.

There are several caveats that should be mentioned with

regard to our result. First, our all-orders perturbative analysis is not sensitive to essential singularities in the coupling constant. However, such essential singularities play no role in the continuum Schwinger model, so we would not expect them to appear in a satisfactory lattice transcription. Furthermore, one can conclude solely on the basis of those parts of the Green's functions that are analytic in the coupling that the DWY theory does not reproduce the continuum results. A second caveat is that our result applies only to a two-dimensional Lagrangian theory. In the case of the Wilson, naive, and Kogut-Susskind derivatives, our analysis of the doubling question would be expected to generalize to higher dimensions. For the DWY derivative, the form of the Rabin smearing function depends critically on the dimensionality of space time and on the details of the Lagrangian. However, based on our two-dimensional analysis, we would expect the behavior of the smearing function merely to determine which of the diseases—doubling, noncovariance, or nonrenormalizable divergences—one will find in the continuum limit.

ACKNOWLEDGMENTS

We wish to thank M. Grady, J. Kogut, P. Nason, J. Rabin, and D. Sinclair for helpful discussions. This work was supported by the U.S. Department of Energy, Division of High Energy Physics, Contract No. W-31-109-ENG-38.

APPENDIX

In this appendix we derive the relation [Eq. (2.20b)] between $G(x,0)$ and $\langle\bar{\psi}\psi\rangle$. The vacuum in the Schwinger model $|\theta\rangle$ is parametrized by an angle θ and satisfies the orthonormality condition

$$\langle\theta|\theta'\rangle=\delta(\theta-\theta') \tag{A1}$$

(Ref. 14). Under a global chiral-symmetry transformation

$$\psi\rightarrow e^{(i/2)(\theta-\theta')\gamma_5}\psi\ , \tag{A2a}$$

the θ vacuum obeys the transformation rule

$$|\theta\rangle\rightarrow|\theta'\rangle \tag{A2b}$$

(Ref. 14). The perturbative vacuum $|0\rangle$ is the chirally symmetric Fourier component of $|\theta\rangle$:

$$|0\rangle=\int_0^{2\pi}d\theta\,|\theta\rangle\ . \tag{A3}$$

Consider the quantity

$$\lim_{x\rightarrow\infty}G(x,0)=\lim_{x\rightarrow\infty}\langle 0|\bar{\psi}\psi(x)\bar{\psi}\psi(0)|0\rangle\ . \tag{A4}$$

We insert a complete set of intermediate states between $\bar{\psi}\psi(x)$ and $\bar{\psi}\psi(0)$. In the limit $x\rightarrow\infty$, only the zero-energy intermediate states (vacuum states) survive—the others being exponentially damped—so we have

$$\begin{aligned}\lim_{x\rightarrow\infty}G(x,0)&=\lim_{x\rightarrow\infty}\int_0^{2\pi}d\theta\langle 0|\bar{\psi}\psi(x)|\theta\rangle\langle\theta|\bar{\psi}\psi(0)|0\rangle\\&=\int_0^{2\pi}d\theta_1 d\theta_2 d\theta\langle\theta_1|\bar{\psi}\psi|\theta\rangle\langle\theta|\bar{\psi}\psi|\theta_2\rangle\ ,\end{aligned} \tag{A5}$$

where in the last line we have substituted Eq. (A3) and made use of the translation invariance of the vacua to drop the explicit x dependence. Now,

$$\langle\theta|\bar{\psi}\psi|\theta'\rangle=\langle\bar{\psi}\psi\rangle\delta(\theta-\theta')\cos\theta\ , \tag{A6}$$

which is the definition of the constant of proportionality $\langle\bar{\psi}\psi\rangle$ (Ref. 14). Substituting Eq. (A6) into Eq. (A5), we obtain the desired result:

$$\begin{aligned}\lim_{x\rightarrow\infty}G(x,0)&=\int_0^{2\pi}d\theta\cos^2\theta\,|\langle\bar{\psi}\psi\rangle|^2\\&=\tfrac{1}{2}|\langle\bar{\psi}\psi\rangle|^2\ .\end{aligned} \tag{A7}$$

This relation was also obtained by Marinari, Parisi, and Rebbi.[22] The result can be derived easily from the fermionic formulation of the Schwinger model as well.[23]

[1]K. G. Wilson, Phys. Rev. D **10**, 2445 (1974); in *New Phenomena in Subnuclear Physics*, edited by A. Zichichi (Plenum, New York, 1977).
[2]J. Kogut and L. Susskind, Phys. Rev. D **11**, 395 (1975).
[3]H. B. Nielsen and M. Ninomiya, Nucl. Phys. **B185**, 20 (1981); **B193**, 173 (1981).
[4]H. B. Nielsen and M. Ninomiya, Phys. Lett. **105B**, 219 (1981).
[5]M. Ninomiya and C.-I Tan, Phys. Rev. Lett. **53**, 1611 (1984); in *QCD and Beyond*, proceedings of the XXth Rencontre de Moriond, Les Arcs, France, 1985, edited by J. Tran Thanh Van (Editions Frontieres, Gif-sur-Yvette, France, 1985).
[6]L. H. Karsten and J. Smit, Nucl. Phys. **B183**, 103 (1981).
[7]S. D. Drell, M. Weinstein, and S. Yankielowicz, Phys. Rev. D **14**, 487 (1976); **14**, 1627 (1976).
[8]M. Weinstein, Phys. Rev. D **26**, 839 (1982).
[9]Helen R. Quinn and Marvin Weinstein, Phys. Rev. D **34**, 2440 (1986).
[10]Jeffrey M. Rabin, Phys. Rev. D **24**, 3218 (1981).
[11]L. H. Karsten and J. Smit, Nucl. Phys. **B144**, 536 (1978).
[12]L. H. Karsten and J. Smit, Phys. Lett. **85B**, 100 (1979).
[13]J. Schwinger, Phys. Rev. **128**, 2425 (1962).
[14]S. Coleman, R. Jackiw, and L. Susskind, Ann. Phys. (N.Y.) **93**, 267 (1975); S. Coleman, *ibid.* **101**, 239 (1976).
[15]J. Lowenstein and J. Swieca, Ann. Phys. (N.Y.) **68**, 72 (1971).
[16]Y. Frishman, in *Particles, Quantum Fields and Statistical Mechanics*, proceedings of the 1973 Summer Institute in Theoretical Physics, Mexico City, 1973, edited by M. Alexanian and A. Zepeda (Lecture Notes in Physics, Vol. 32) (Springer, Berlin, 1975).
[17]S. L. Adler, Phys. Rev. **177**, 2426 (1969); W. A. Bardeen, *ibid.* **184**, 1849 (1969).
[18]Belal E. Baaquie, J. Phys. G **8**, 1621 (1982).
[19]J. B. Kogut, Rev. Mod. Phys. **55**, 775 (1983).
[20]G. Grammer, Jr. and D. R. Yennie, Phys. Rev. D **8**, 4332 (1973).
[21]N. Mermin and H. Wagner, Phys. Rev. Lett. **17**, 1133 (1966).
[22]E. Marinari, G. Parisi, and C. Rebbi, Nucl. Phys. **B190**, 734 (1981).
[23]G. T. Bodwin and E. V. Kovacs (in preparation).